MASTER THESIS

Characterization of an acetogenic industrial flue gas fermentation process with *Acetobacterium woodii*

carried out for the purpose of obtaining the degree of Master of Science (MSc or Dipl.-Ing. or DI), submitted at TU Wien, Faculty of Mechanical and Industrial Engineering, Institute of Chemical, Environmental & Biological Engineering (Head: Univ.Prof. Dipl.-Ing. Dr.techn. Anton Friedl), by

Florian NIEDERBERGER, BSc
01126639

Supervisor:

Univ.Prof. Dipl.-Ing. Dr.techn. Christoph Herwig

Univ.Ass. Dipl.-Ing.(FH) Dr. Stefan Pflügl

Date:

24. October 2017

Acknowledgements

I want to thank everybody who supported me throughout this master thesis.

I especially want to thank Prof. Christoph Herwig for the opportunity to work in his research group. He provided such a professional yet warm and friendly atmosphere within the group and it was a great honour to work with his supervision.

I also thank my supervisor Stefan Pflügl for his expertise, sincere and valuable guidance and ecouragement extended to me.

A big thank you to my research colleagues Anna, Julianne, Paul, Franzi, Luis, Katharina, Andrea and Lukas who where always there to give good advice.

My sense of gratitude goes to all who, directly and indirectly, have lent their helping hand in the laboratory and in this piece of work.

Last but not least I want to thank my family, my partner Selina, friends and colleagues who supported me during my studies and made a major contribution towards the successful completion of my studies.

I confirm, that going to press of this thesis needs the confirmation of the examination committee.

Affidavit

I declare in lieu of oath, that I wrote this thesis and performed the associated research myself, using only literature cited in this volume. If text passages from sources are used literally, they are marked as such.
I confirm that this work is original and has not been submitted elsewhere for any examination, nor is it currently under considerations for a thesis elsewhere.

Vienna, _____   _____

             Date   Signature

Abstract

The increasing concerns and activities around global climate change induced new energy and emission policies. High industrial emissions must be targeted to lower the carbon dioxide impact.

The focus of this work is on the first step of a two step biotechnological process with industrial flue gases containing hydrogen, carbon dioxide, carbon monoxide, oxygen, nitrogen and methane for conversion into valuable products. An autotrophic fermentation process with *Acetobacterium woodii* was characterized and described. The utilized facultative anaerobic bacteria *Acetobacterium woodii* is known for growing chemolithoautotrophically on carbon dioxide and hydrogen with acetate as the sole product.

Batch and chemostat cultivations were applied to study different influences such as mass transfer, specific reaction rates and productivity. Due to inadequate mass transfer the process was identified as hydrogen limited . Final acetate concentrations of 25 g/L were measured at low biomass concentrations of 0.8 to 1.2 g/L in less than five days under autotrophic conditions. The highest accomplished biomass specific reaction rate was 13.20 g/g d.

Small scale serum bottle experiments were used to evaluate inhibitory effects of carbon monoxide and oxygen. Contradictory results were obtained from these tests. Furthermore, online calculators and possible online sensoring (within the process information management system Lucullus) for solid online process screening were evaluated. This led to effective on-line acetate monitoring via a soft sensor based on the base signal.

Contents

Contents

A. Appendix I

List of Figures

List of Tables

Abbreviations

Abbrevation	Unit	Description
A	m^2	area
CDTR	mol/L h	carbon dioxide transfer rate
CDUR	mol/L h	carbon dioxide uptake rate
CDW	g/L	cell dry weight
c_i*	g/L	equilibrium concentration of component i
c_i	g/L	concentration of component i
$c_{i,0}$	g/L	concentration of component i at t=0
C_i	K	temperature coefficient
CSTR		continuous stirred tank reactor
D_i	1	diffusion constant of component i
D	1/h	dilution rate
D_c	1/h	critical dilution rate
DoE		Design of Experiment
DoR	1	degree of reduction
H_i	mol/L bar	Henry constant
HTR	mol/L h	hydrogen transfer rate
HUR	mol/L h	hydrogen uptake rate
$k_L a$	1/s	volumetric transport coefficient

K_S	g/L		saturation constant of limiting substrate
μ	1/h		specific growth rate
OD_{600}	AU		optical density at 600 nm
OD_{880}	AU		optical density at 880 nm
p_i	bar		partial pressure
$q_{i/j}$	g/g h		specific rate of component i specific to j
			(if not stated different specific to X)
R	J/mol K		gas constant
r_i	g/L h		volumetric reaction rate of component i
STR			stirred tank reactor
V	m^3		volume
$\dot{V}$	L/h		volumetric flowrate
V_R	L		reactor volume
Δx	m		thickness of laminar liquid boundary layer
$Y_{i/j}$	g/g		yield of component i specific to j

1. Introduction

The increasing concerns and activities around global warming and climate change over the last decade lead to political and public debates which induced new energy and emission policies (COP 21/Global, Renewable Energy Roadmap 21/European Commission). In 2016, the United Nations Framework Convention on Climate Change, 21st Conference of the Parties (COP 21 Paris Agreement) set global goals to slow down and stop anthropogenic climate change. These goals were set to limit the maximum global temperature rise to well below 2 °C in comparison to pre-industrial levels and included the progressive reduction and complete stop of greenhouse gas emissions between 2045 and 2060, the transition of the energy supply (e.g. electricity, heat and transport) based entirely on renewable sources and a partial removal of already emitted carbon dioxide from earths atmosphere [21]. Big economical, environmental and scientific efforts aim to preserve modern and technical achievements but in a sustainable and carbon/CO_2 neutral way.

A complex combined system of renewable energy sources, storage systems and low or zero emission industrial plants must evolve and interact in a symbiotic way [26]. The widespread construction of diverse renewable energy sources all over Europe (e.g. Offshore wind parks, concentration solar power plants) though leads to a problematic phenomena. Different energy storing technologies to use or consume excess energy peaks and provide a constant power supply are needed. Various solutions are possible and feasible, but it is expected that a variety of technologies must interlink to incorporate the geographical possibilities and diversity across Europe [21].

Nevertheless not all conventional processes work in a carbon neutral way, e.g. calcination of lime stone for cement or the metallurgical conversion of ores to refined

metals such as iron, steel or copper. This leads to unavoidable emissions of mainly CO and CO_2. Despite efforts to reduce emissions (approx. 52 % reduction over the last decade), iron and steel production remains the biggest industrial emitter of greenhouse gases in the European Union [21]. Therefore a closed carbon cycle system in the chemical industry is necessary to significantly enhance sustainability. Manufacturing waste or flue gases could be used as a feedstock for the production of energy and chemicals without competing with food resources. In general this would lead to a reduction of the CO_2 impact. This would be especially vital in the metallurgical and cement industries mentioned above. Also the overall carbon recovery of conventional sugar based fermentation could be improved with anaerobic, autotrophic organisms and finally little or no carbon dioxide would be emitted [48]. The cleaned (particular matter) and purified CO_2 and/or CO containing flue gas could be converted with hydrogen to value added products. The H_2 can originate from coke oven gas, neighbouring industries or most preferably from water electrolysis of excess renewable energy sources mainly wind, solar and hydroelectrical power. This is also known as Power-to-Product, a chemical storage of excess electrical energy. Anaerobic biochemical fermentation, catalytic reaction or electro-chemical transformation could be used as conversion methods.

1.1. Process concept

This research project aims to produce valuable products such as base chemicals and fuels from carbon dioxide, carbon monoxide and hydrogen containing industrial flue gas. In addition, excess renewable energy should be stored by utilizing hydrogen, which originates from e.g. water electrolysis. This work, as part of this project, is focused around the first step of a two step biotechnological process.

In the first step carbon containing flue gases and hydrogen is converted to acetate as the main product, as well as biomass with traces of formate. The anaerobic acetogen *Acetobacterium woodii* is used for this initial carbon fixation. Acetate serves as an intermediate for further processing. It already stores the chemical energy of hydrogen
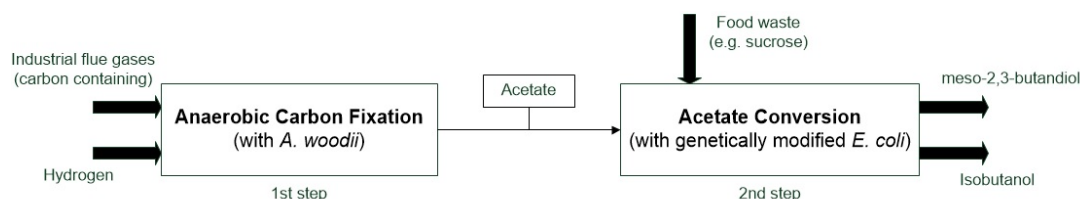
Figure 1.1.: Flow chart of the two step process

as described above in the Power-to-Product concept.

In the following process step, either the purified acetate or directly the cultivation broth from the first step is converted into meso-2,3-butandiol or isobutanol with genetically modified *Escherichia coli*. This includes metabolic engineering of *E. coli* to incorporate a 2,3-butanediol production pathway from natural producers and a synthetic isobutanol production pathway.

Furthermore the process development of an efficient co-utilization of acetate with CO_2/formate, sugars (e.g. glucose) or other substrates (food-based material possibly including sucrose) without or with small formation of CO_2 and suitable fermentation conditions (e.g. aeration modes) are researched.
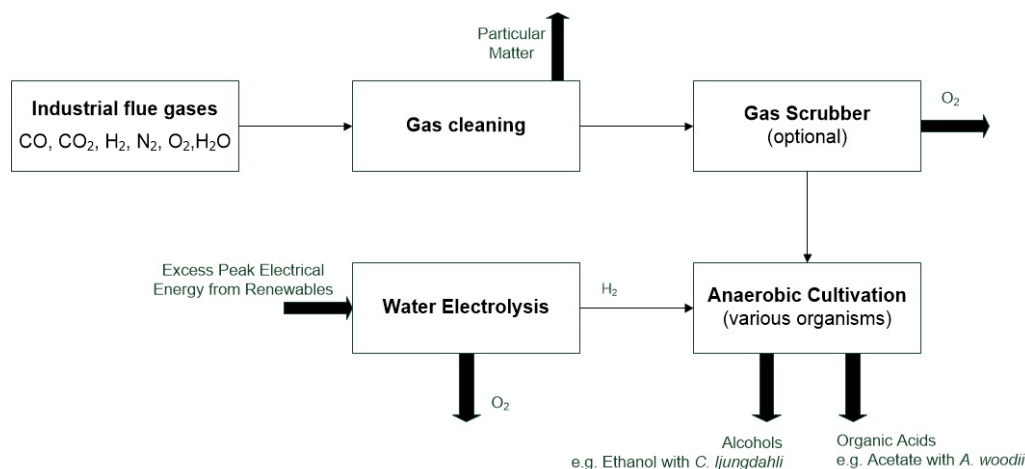
Figure 1.2.: First step of process scheme in more detail

This two step system benefits from its more variable approach towards design and process development as well as product diversity. The initial fixation step is independent from the second step and therefore could be designed specifically for different flue and waste gas compositions. Additionally, the second step could be performed

for different end products at higher efficiency in a parallel reactor approach. Every organism capable of utilizing acetate would be suitable and would further enlarge the potential product portfolio of a biorefinery. A following chemical conversion step of the alcohols could produce a fossil resource equivalent fuel for standard known applications. Decreasing fossil resources and potentially increasing crude oil prices could lead to an effective solution in contrast to the fossil competition.

An additional benefit of this Power-To-Product storage process lies in the physical properties and easy utilization of the end product. The high energy density of liquid fuels is unbeaten by other techniques such as thermochemical storage or hydrogen storing tank systems. In addition to most of the current techniques for energy supply, distribution (e.g. heating) and transport means as well as chemical base commodities are based around hydrocarbons. Therefore safe and easy handling, transport and storage is an industrial standard for these chemicals.

There are commercial size biochemical fermentation plants under construction in Asia and Europe (e.g. China Shougang Group, LanzaTech and in Belgium Arcelor-Mittal) and pilot plants located within steel mills. They use steel mill waste gases (similar composition to syngas) to produce ethanol. Furthermore, processes have been developed for the synthesis of jet fuels with anaerobic acetogenic bacteria [48]. There are currently no known and published industrial or pilot plant applications for acetic acid or acetate production with *A. woodii* on flue gases.

In addition, industrial waste and flue gas utilization for acetogenesis is only specified for components such as hydrogen and carbon dioxide.

> "Similarly, the gaseous substrate may be a CO_2 and H_2 containing waste gas obtained as a by-product of an industrial process, or from some other source." -US Patent 9068202 [40]

1.2. Scientific Question

The aim of this work was to develop and characterize the first step of the above described biotechnological process for the efficient and continuous fixation of carbon dioxide from idealized and real industrial flue gas. Figure 1.3 shows the essential prerequisites for a successful bioprocess development [52].
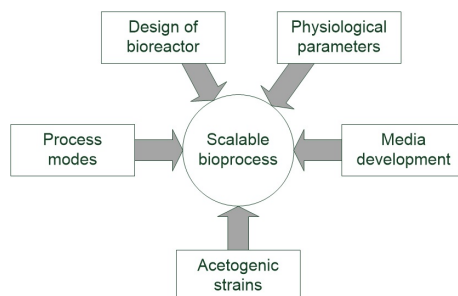
Figure 1.3.: Requirements for bioprocess development and scale up. Figure adapted from [52]

This work particularly discusses the following: What is the influence of gas mixtures corresponding to real industrial flue gases towards growth and productivity ($q_{acetate}, r_{acetate}$) of *Acetobacterium woodii* in comparison to gas mixtures with the stoichiometric optimum?

What are potential inhibitors in the real gas mixtures and how does *A. woodii* respond to them?

Furthermore, what are the influences of cultivation mode and condition on performance and where is the optimum?

A comprehensible and sustainable way for further process improvement and potential scale-up such as on-line data processing and soft sensor applications were applied for solving these tasks.

2. Theory

2.1. Acetogenic microorganisms

All known species of acetogenic bacteria belong either to the gram positive bacteria *Firmicutes* or to a group of the recently discovered anaerobic *Spirochaetes* [24], [41]. Acetogenic microorganisms from the genus *Clostridium* and *Acetobacterium* are capable of producing acetic acid, ethanol and other fermentation products under strictly anaerobic conditions from different substrates [30]. Acetogens can grow by oxidizing a variety of organic substrates, e.g. hexoses, pentoses, alcohols or by oxidation of inorganic substrates such as hydrogen or carbon monoxide coupled with the reduction of carbon dioxide [57]. This makes acetogens facultative autotrophs. The metabolic pathway flexibility originates from the ecological competition with mainly methanogenic organisms. Due to their lower H_2 threshold and the greater energy yield of the CO_2 and H_2 to methane conversion, acetogens must often evade to different metabolic pathways [51].
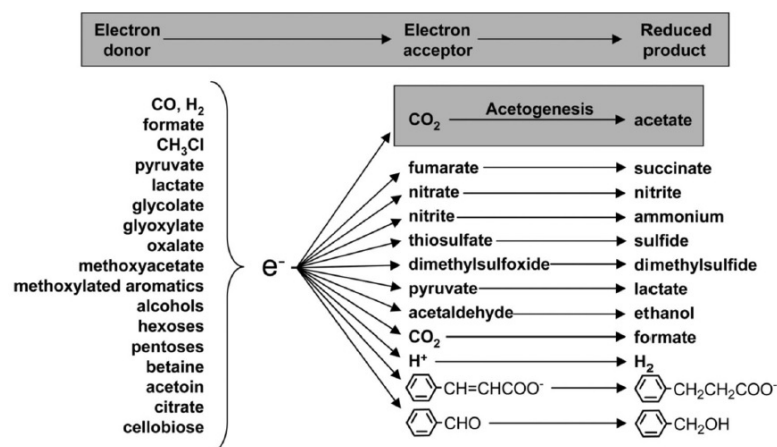
Figure 2.1.: Redox couples that can be used by acetogens. Figure taken from [51]

This diversity of applicable substrates for acetogenentic microorganisms would allow for the use of food waste and sugar streams in combination with flue and synthesis gas for acetogenesis.

2.1.1. Heterotrophic pathway

Acetogenic microorganisms are capable of converting organic carbon sources anaerobically to acetate as the sole end product. This conversion is also called homoacetogenesis [57].
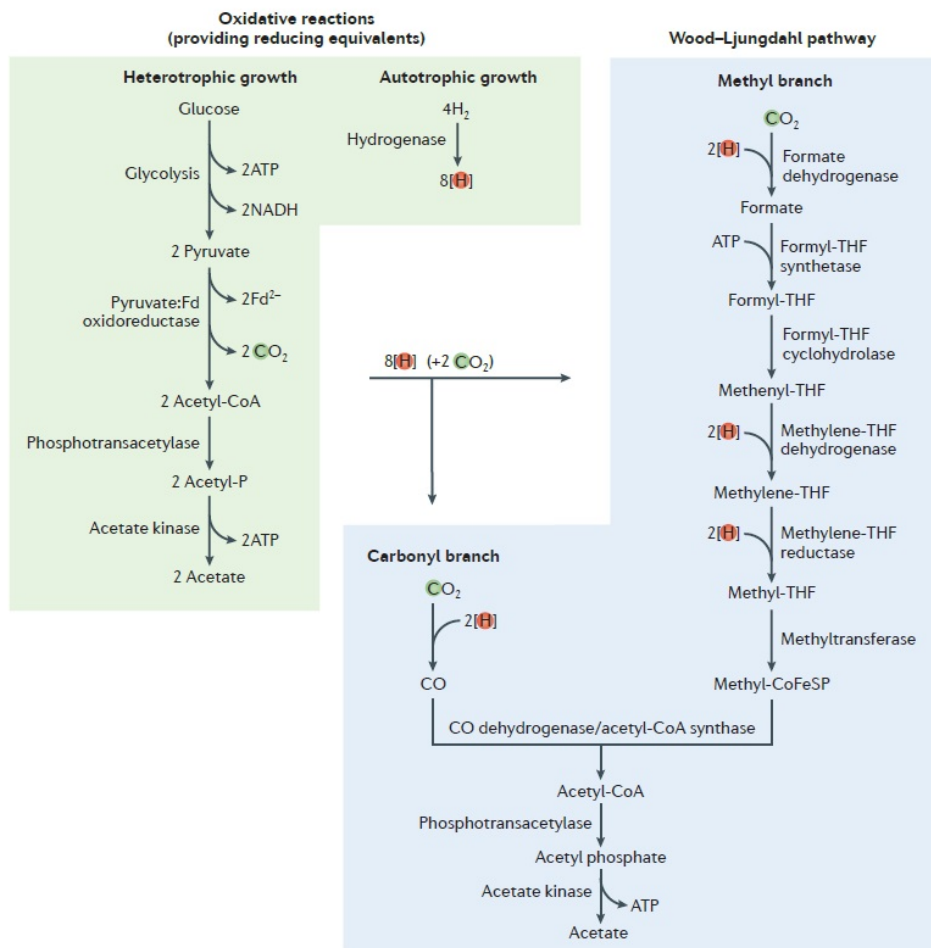
Figure 2.2.: Metabolic pathways of acetogenesis. Figure taken from [57]

One mol hexose (e.g. glucose and fructose) is converted via glycolysis (Embden-Meyerhof-Parnas pathway) to two mol pyruvate, two mol ATP and four mol redox-equivalents [H]. The pyruvate is decarboxlized to two mol acetyl-CoA and CO_2. Additional four mol redox-equivalents are produced through the pyruvate:ferredoxin

oxidoreductase. Phosphotransacetylase and acetate kinase transform acetyl-CoA further to two mol acetate and two mol ATP. All four mol ATP emerge from substrate level phosphorylation [57]. The produced two mol CO_2 and eight mol redox-equivalents are converted to a third mol acetate via the autotrophic Wood-Ljungdahl pathway, which is described in more detail below [51], [64]. The left part of figure 2.2 shows this mechanisms.

The stoichiometric conversion of glucose to acetate is shown in equation (2.1) [51].

$$C_6H_{12}O_6 + 4\,ADP + 4P_i \rightarrow 2\,CH_3COOH + 2\,CO_2 + 4\,ATP + 8\,H^+ + 8\,e^- + 2\,H_2O$$
$$2\,CO_2 + 8\,H^+ + 8\,e^- \rightarrow CH_3COOH + 2\,H_2O$$
$$\overline{C_6H_{12}O_6 + 4\,ADP + 4\,P_i \rightarrow 3\,CH_3COOH + 4\,ATP + 4\,H_2O} \qquad (2.1)$$
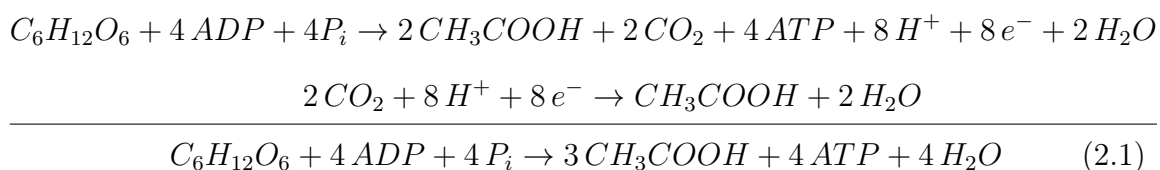
2.1.2. The Wood-Ljungdhal pathway

The Wood-Ljungdhal pathway couples energy conservation and CO_2 fixation and it is the central metabolism for acetogens to grow autotrophically [51]. The stoichiometry of the reduction of CO_2 to acetate is as seen in equation (2.2).

$$4\,H_2 + 2\,CO_2 \rightarrow CH_3COOH + 2\,H_2O \qquad (2.2)$$
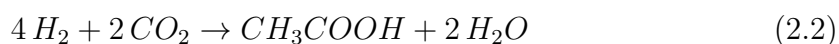
The Wood-Ljungdhal pathway consists of two seperate branches, a carbonyl and a methyl branch, each is responsible for the reduction of one mol carbon dioxide (from equation (2.2)) [57].

In the methyl branch one mol CO_2 is reduced to formate via a formate dehydrogenase and the consumption of two mol redox-equivalents [H]. One mol ATP is utilized in the binding step of the formyl group to the cofactor tetrahydrofolate. Ensuing it is reduced stepwise to one mol methyl-tetrahydrofolate with four mol redox-equivalents [39]. Another mol of CO_2 and two mol redox-equivalents are reduced to CO in the carbonyl branch. The bifunctional CO dehydrogenase/acetyl-CoA synthase fuses the carbonyl group and methyl group from the two branches and CoA to one mol acetyl-CoA. One mol ATP via phosphotransacetylase and acetate kinase is recovered, while the acetyl-CoA is turned into one mol acetate [57]. The right part of figure

2.2 shows this mechanisms. In the Wood-Ljungdahl pathway no net synthesis of ATP is possible [39], [51]. The energy conservation will be discussed in the following section.

2.1.3. Energy conservation in acetogenic bacteria

The universal energy carrier in every living cell is ATP (adenosintriphosphate) which transports chemical energy within cells for metabolism. Two options to generate ATP are known: substrate level phosphorylation and chemiosmotic ion gradient-driven phosphorylation [57].

For the production of ATP the substrate level phosphorylation combines a chemical reaction, directly with the phosporylation of ADP. The exact number of produced ATP molecules vary and depends on the bacterial strain and conditions [15].

As a counterpart chemiosmotic ATP production links an exergonic reaction, mostly an electron-transfer reaction to the translocation of ions through a membrane to generate an ion and/or electrical gradient which propels ATP synthesis via a membrane bound synthase [57] [6].

Microorganisms which utilize the acetyl-CoA-pathway for autotrophic CO_2 fixation rely on the chemiosmotic energy conservation.

From a bioenergetic point of view acetogenic micororganisms were divided into two groups for a long time, a H^+-dependent and a Na^+-dependent group [45]. The groups differ not only in the sort of gradient, but in the composition of the membrane-bound electron transport chain [15]. *Moorella thermoacetica* is a H^+- dependent (Na^+-independent) cytochrome-containing and *A. woodii* a Na^+-dependent and cytochrome free model organism for each group [57].

The impossible classification of *Clostridum ljungdahlii* into those groups led to a different grouping suggested by Schuchmann et.al. [57]. Acetogenic microorganisms contain either a Rnf-complex (a Ferredoxin-NAD^+ oxyreductase) or an Ech-complex (an energy conserving hydrogenase) and are still classified into sub groups due to the involved ions [57].

2.2. *Acetobacterium woodii*

Acetobacterium woodii (family: *Eubacteriaceae*) was discovered and isolated from black sediment of Oyster Pond inlet (Woods Hole, MA, USA) in 1977 [3]. It is a 1-2 μm long, gram-positive, non-spore forming oval rod-shaped bacterium which often occurs in pairs and has the ability to move actively with one or two subterminal flagella (Figure 2.3) [57]. As a mesophilic organism *A. woodii* shows optimal growth at 30 °C and neutral pH [3].

It is known to grow chemolithoautotrophically on hydrogen and carbon dioxide and chemoorganoheterotrophically on e.g. fructose, glucose, lactate, glycerol and formate [2],[3]. Furthermore mixotrophic growth, i.e. combined utilization of carbon dioxide as well as organic compounds, was reported [11],[15]. *A. woodii* is a representative of the homoacetogens, which means that acetate is the main end product.[2],[36].
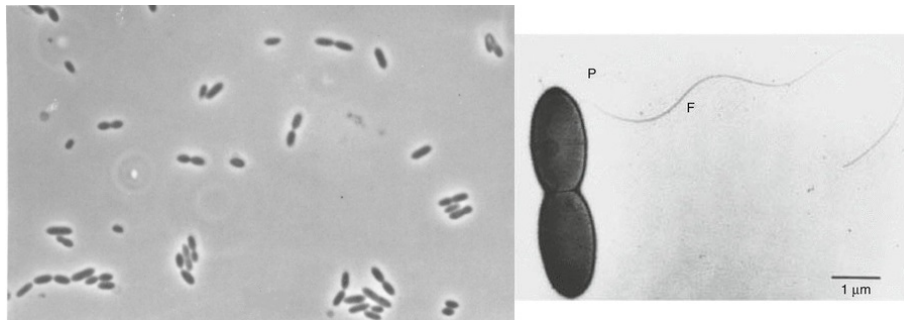
Figure 2.3.: Left: Phase contrast photomicrograph of *A. woodii*, Right: Electron micrograph of *A. woodii* with a single, subterminal flagellum F and pili-like structures P. Figures taken from [3]

A. woodii embodies a Rnf complex and a Na$^+$ translocating F_1F_0 ATPase and is therefore classified into the group of Rnf- and sodium dependent acetogens [23].

In addition, the analysis of the genome sequence revealed that all enzymes of the Wood-Ljungdahl pathway, except the Na$^+$ translocating and membrane-bound F_1F_0 ATPase, as well as the hydrogenases are soluble [8], [23].

The reductive branch of the acetogenesis utilizes one mol hydrogen directly as an electron donor for the carbon dioxide reduction with the hydrogen-dependent CO_2 reductase (HDCR) [57]. The oxidation of the remaining three mol H_2, as electron donor, via the electron-bifurcating hydrogenase (HydABCD) results in 1.5 mol
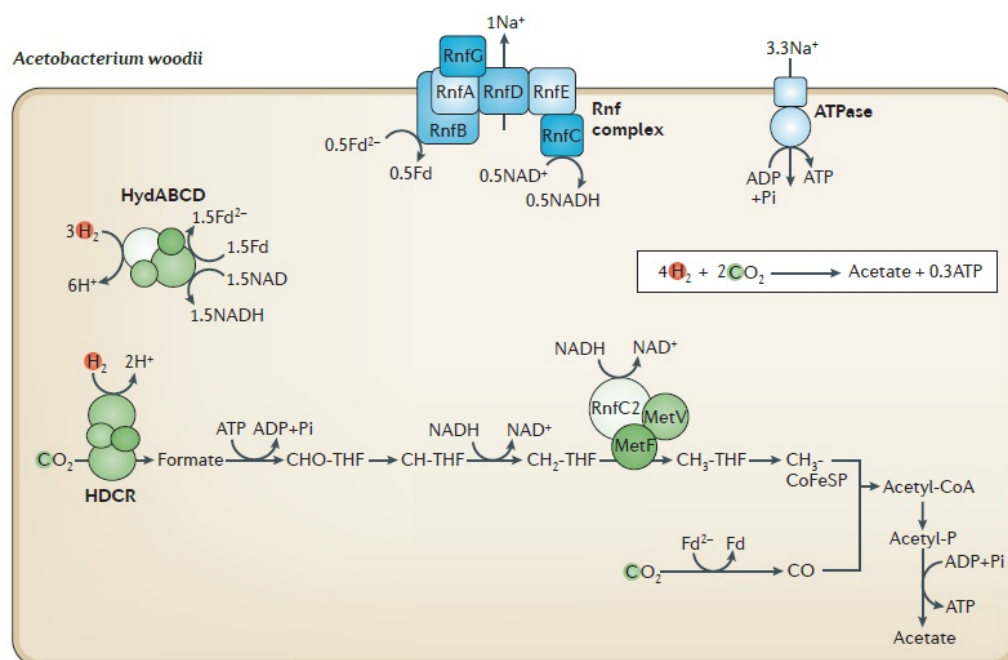
Figure 2.4.: Model of acetogenesis in *A. woodii*. Figure taken from [57]

reduced ferredoxin (Fd^{2-}, endergonic reduction) and 1.5 mol NADH (exergonic reduction). In relation to the CODH/ACS reaction one mol Fd^{2-} is used to reduce one mol CO_2 to CO. The excess 0.5 mol Fd^{2-} is oxidized by the Rnf complex which reduces 0.5 mol NAD^+ to 0.5 mol NADH and builds up the necessary chemiosmotic Na^+ gradient. This gradient drives ATP synthesis via the Na^+-dependent ATPase [6]. The remaining two mol NADH are used in the methyl branch of the Wood-Ljungdahl pathway to reduce one mol each methenyl-THF and methylene-THF [57]. In total, 0.3 ATP could be synthesized per mol acetate produced [6], [57]. This mechanism is illustrated in figure 2.4.

2.2.1. Important enzymes

Ferredoxin

Ferredoxins are small proteins containing iron and sulphur which work as the physiological electron acceptors for hydrogenases [1]. They are involved in many reactions of the anaerobic metabolism for electron transport and therefore it is crucial for the cell to keep ferredoxin in a reduced state [8]. Ferredoxin represents the connection

between glycolysis and the WLP and therefore can be seen as a key enzyme of the metabolism [57].

Hydrogenases

Acetogens need utilizable energy (electrons and reduction equivalents) which originates from enzymatic conversion of gaseous hydrogen by hydrogenases. Therefore hydrogenases are linked together with the redox equilibrium in the cell [14].

Different to most other acetogens the hydrogenases are at maximum activity in *A. woodii* independent from the type of substrate they use compared to other acetogens [14]. This enables the simultaneous utilization of both substrates, also called mixotrophy [11].

A known inhibtor of this enzyme is CO. Studies have shown that for H_2 and CO containing gas, CO is used prior hydrogen uptake starts, which can be explained by the reduced hydrogenase activity [7].

Carbonic anhydrase/Acetatetransport

Carbonic anhydrase is a zinc-containing enzyme which catalyses the reversible hydration of CO_2 to HCO_3^- very efficiently [12]. This was indicated in many acetogens, due to the fact that they have a high demand of CO_2 during autotrophic growth and therefore play a decisive role as well. *A. woodii* was shown to have the highest activity for carbonic anhydrase among acetogenic microorganisms [12].

Carbonic anhydrase could also regulate the intracellular pH coupled with a acetate/HCO_3^- antiporter [12]. Active export of acetate from the cell was shown, although the detailed transport proteins are unclear [10].

2.3. Basics of bioprocess engineering

In this section the concepts of mass balancing of the stirred tank reactor (STR) in different modes as well as growth and product formation of microorganisms will be exemplified.

2.3.1. Kinetics of product formation and growth

The mathematical contemplation of cell cultures in bioreactors are described as a uniform component, without any subpopulations or distinguishable elements, and certain cell properties as a median [13]. Thereby main kinetic parameters for growth and product formation can be defined easily.

The specific growth rate μ and growth rate r_X describe the change of biomass over time and are therefore important process parameters. For non-limited conditions they are defined as follows:

$$\mu = \frac{1}{c_X} \cdot \frac{dc_x}{dt} \tag{2.3}$$

$$r_X = \frac{dc_X}{dt} = \mu \cdot c_X \tag{2.4}$$

Monod (1949) described a relation between specific growth rate and the growth limiting substrate (usually the carbon source in defined media) [13], [36]. Due to this model the maximum growth rate is reached when the substrate concentration c_S is much higher than the saturation constant K_S.

$$\mu = \mu_{max} \cdot \frac{c_S}{c_S + K_S} \tag{2.5}$$

A similar description as for the biomass rates (equation (2.3)) is suitable for the volumetric r_i and cell specific rates q_i of product formation and substrate utilization.

$$r_S = \frac{dc_S}{dt} = q_S \cdot c_X \tag{2.6}$$

$$r_P = \frac{dc_P}{dt} = q_P \cdot c_X \tag{2.7}$$

The biomass and substrate concentrations can be correlated via the biomass yield $Y_{X/S}$, the amount of produced biomass per consumed substrate. It can also be denoted as selectivity [13].

$$Y_{X/S} = \frac{produced\,biomass}{consumed\,substrate} = \frac{r_X}{r_S} = \frac{dc_X}{dc_S} \tag{2.8}$$

Product formation is strongly interlinked with the physiologic importance of the product in the metabolism of the cell [13]. The product yield is one of the main factors for the evaluation of economic value and efficiency of the process. It correlates the amount of formed product per consumed substrate [13].

$$Y_{P/S} = \frac{formed\,product}{consumed\,substrate} = \frac{q_P}{q_S} = \frac{r_P}{r_S} = \frac{dc_P}{dc_S} \tag{2.9}$$

2.3.2. Integral balancing of the ideal stirred tank reactor

The ideal stirred tank reactor (STR) is an ideal model for all fluids to estimate and calculate important process variables. An ideal mixture of each fluid element in the reactor is assumed and therefore the concentrations for each species is constant, regardless of dissolved gases in the liquid phase or different liquid components [13]. A biological reactor is an enclosed unit operation for material conversion in the presence of a biocatalyst. The mainly performed tasks are mixing of the fluid for homogeneous condition and for better transport of nutrients and gaseous components to the cells. As a special requirement, different from other chemical reactors, a sterile environment must be assured [36].

Under the assumption of isothermal and isobaric conditions the general material balance for the STR can be written as following:

$$In - Out + Reaction = Accumulation \tag{2.10}$$

$$\dot{V}_{In} \cdot c_{i,In} - \dot{V}_{Out} \cdot c_{i,Out} + V_R \cdot r_i = V_R \cdot \frac{\partial c_i}{\partial t} + c_i \cdot \frac{\partial V_R}{\partial t} \tag{2.11}$$

2.3.2.1. Batch processing in an ideal stirred tank reactor

For a batch process all needed media components are already in the reactor and therefore it is a closed systems for the liquid phase (no Ins and Outs in figure 2.5). Despite little additions of pH control via base or acid and other additives (e.g. antifoam), the reaction volume V_R can be assumed as constant [13]. However, required gaseous components are added continuously. In bioprocess engineering it is still idealized as a closed systems.
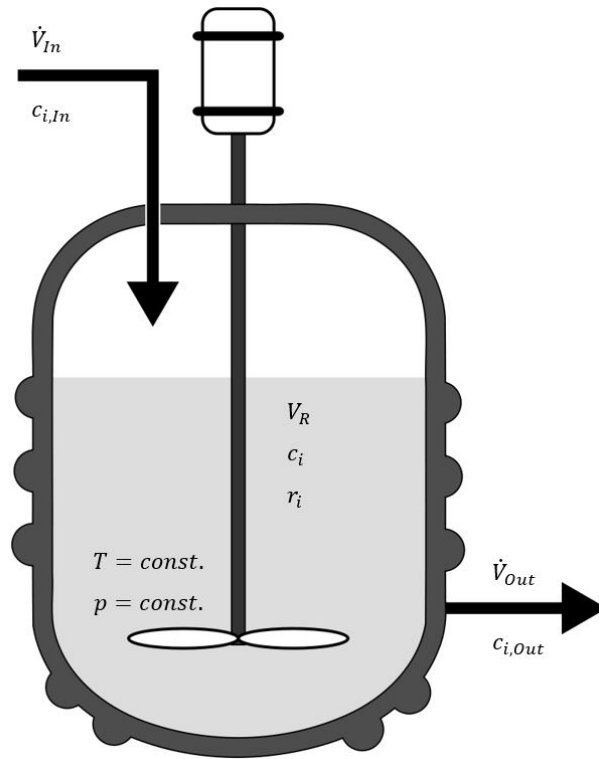
Figure 2.5.: Scheme of an isothermal and isobaric contionous stirred tank reactor (CSTR)

Due to a proper agitation spatial constant process properties (concentration, physical properties, reactions rates, etc.) are assured. Therefore the general balance (2.10) is reduced to

$$V_R \cdot r_i = V_R \cdot \frac{\partial c_i}{\partial t} \tag{2.12}$$

and further leads us to the reaction rates.

$$r_i = \frac{dc_i}{dt} \tag{2.13}$$

Consequently, measurements of the concentration changes over time lead to the corresponding rates.

Microbial growth in batch cultivations can be divided into different phases (figure 2.6). After inoculation the microorganisms require a certain time to adapt to the current process conditions (Lag-phase). Afterwards exponential maximum repro-

duction with a maximum growth rate μ_{max} can be observed [24], [13].
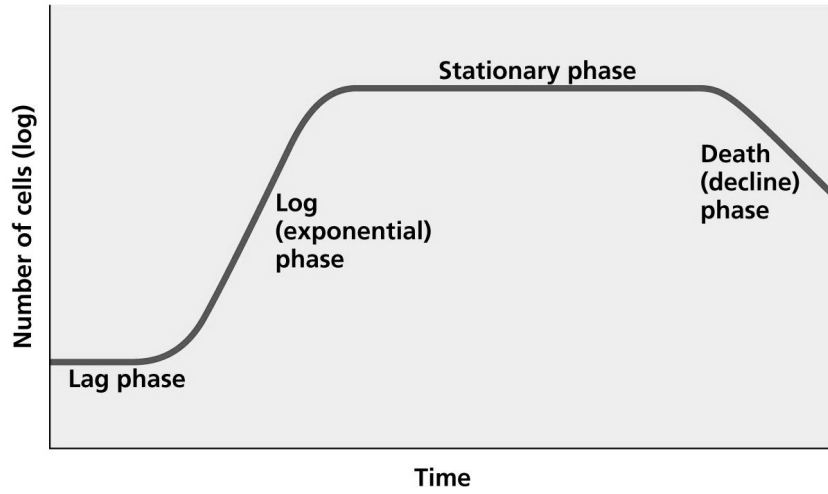
Figure 2.6.: Growth phases of microorganisms in batch cultivations. (Copyright 2006 Pearson Education, Inc., published Benjamin Cummings)

Under the assumption of a constant growth rate during the exponential phase equation (2.3) can be integrated and rearranged for an easy evaluation of the growth rate from the measured data.

$$c_X = c_{X,0} \cdot e^{\mu_{max} \cdot t} \tag{2.14}$$

$$ln\left(\frac{c_X}{c_{X,0}}\right) = \mu_{max} \cdot t \tag{2.15}$$

Following, after consumption of one or more substrates or an inhibition, a stationary phase with mainly maintenance metabolism and a balance between growth rate and death rate is reached. Ensuing the mortality increases, the cells start to lyse and resulting in a decreased biomass concentration. [24], [13].

2.3.2.2. Ideal continous stirred tank reactor - Chemostat

An ideal mixture of each fluid element in the reactor is assured and therefore the concentrations for each species in the reactor is constant and equal to the outflow of the reactor. The continuous mode of an ideal stirred tank reactor is characterized with a feed of media and removal of culture broth. If there are inequalities the reaction volume is either increased or decreased. Furthermore, if the dilution rate

exceeds the growth rate the biomass concentration decreases gradually and could result in a cell wash out [13]. When both flows are adjusted equally ($\dot{V}_{In} = \dot{V}_{Out} = \dot{V}$) a flow equilibrium can be established and thereafter equation (2.10) is reduced to

$$\dot{V}_{In} \cdot c_{i,In} - \dot{V}_{Out} \cdot c_{i,Out} + V_R \cdot r_i = 0 \tag{2.16}$$

and the dilution rate D can be defined as:

$$D = \mu = \frac{\dot{V}}{V_R} \tag{2.17}$$

Thus equation (2.16) is reduced to

$$r_i = -D \cdot (c_{i,In} - c_{i,Out}) \tag{2.18}$$

and with a sterile, biomass free feed the following equation 2.18 results in

$$r_X = D \cdot c_X \tag{2.19}$$

and is further combined with equation (2.4) to

$$\mu = D \tag{2.20}$$

As an obvious result the chemostat allows us to specify the growth rate through the dilution rate.

A similar description can be derived from equation (2.18) for the volumetric rates under the assumption, that there is no product in the feed media.

$$r_S = -D \cdot (c_{S,In} - c_{S,Out}) \tag{2.21}$$

$$r_P = D \cdot c_{P,Out} \tag{2.22}$$

Due to the organism- and process- dependent maximum growth rate μ_{max}, the dilution rate can be increased until the substrate concentration reaches a maximum ($c_{S,In} = c_S$). This limit is attained when there is no biomass left and is therefore

called the critical dilution rate D_c [13]. The correlation between dilution rate and biomass concentration is shown in figure 2.7. Furthermore the volumetric biomass formation rate r_X, also called productivity, in the chemostat is displayed.
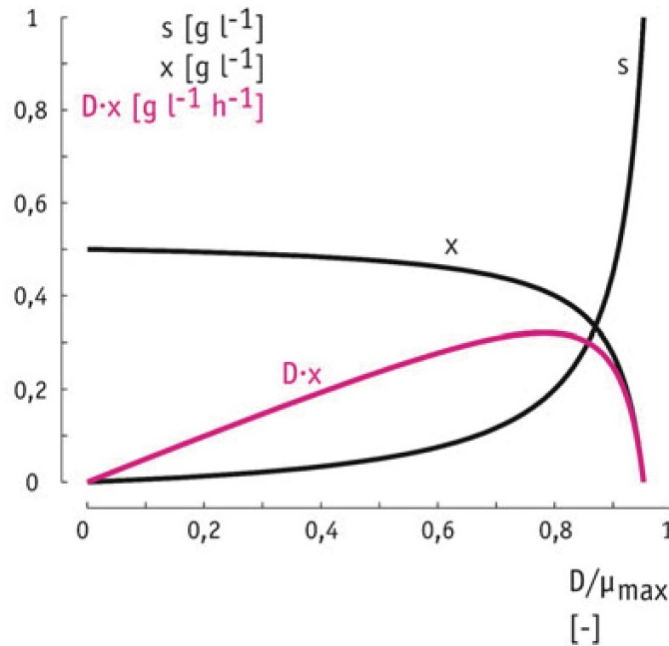
Figure 2.7.: Qualitative X-D diagram normalized to μ_{max}. Figure taken from [13]

The optimal dilution rate would be at the maximum of the r_X- curve and therefore equal to maximum productivity. An on-line turbidity probe could help sustain that optimum. A process near D_c should be avoided due to unstable process conditions and a potential cell wash-out [13].

2.4. Gas-liquid mass transfer

When biological processes are supplied with gaseous substrates, the transfer rate into the liquid phase is the centerpiece for a proper gas feed of the cells. In general, the gas-liquid mass transfer is a limiting step in bioprocesses. The big differences in gas solubilities (see figure 2.9) as well as the fact that gas is the only substrate for autotrophic cultivations, the mass transfer limitation issues are even more distinct [17].

Therefore, the transfer rate should always exceed the cellular uptake rate for gaseous

substrates to avoid limitations, but there are various transport resistances for the gas molecules to overcome from the gas bubble until the utilization in the cell [53]. The different steps are illustrated in figure 2.8.

(1) transfer inside the bubble to the boundary layer

(2) transport through the gas-liquid boundary layer

(3) diffusion through the laminar fluid layer around the gas bubble

(4) transport in the well-mixed fluid

(5) diffusion through the laminar fluid layer around the cell

(6) diffusion across the cell membrane

(7) intracellular transport to reaction centers
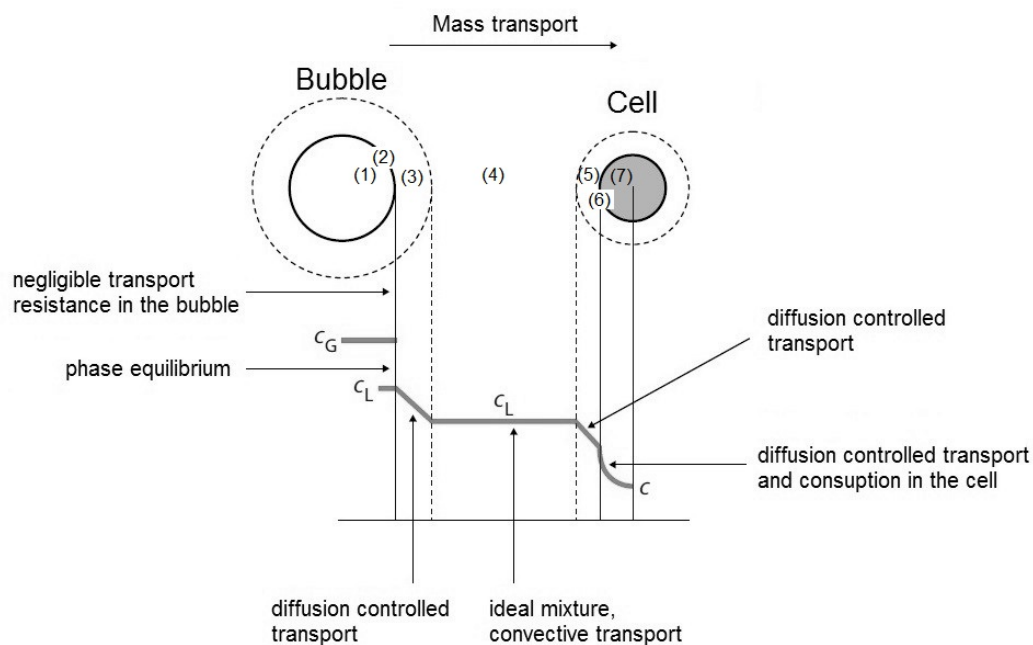
Figure 2.8.: The path of gaseous substrates from the bubble and the surrounding boundary layer through the ideally mixed liquid to the cell with c_L (concentration change of dissolved gas) and c_G (concentration in gaseous phase) and the trend of the concentrations

The mass transfer rate is affected by various factors, such as the size of bubbles and cells, the mixing regime in the bioreactor and the rheological fluid properties [13].

In a typical bioreactor setup the main resistance originates from the transfer of gas molecules through the surrounding boundary layer of the gas bubble.

That rate-determining step can be described with three models [53]:

- two film theory

- penetration model

- model of the surface replacement

The two film theory is used most frequently for the description of transport phenomena of boundary layers and is therefore explained in more detail [13].

The two film theory is based on Fick's first law. It is assumed, that there is a thermodynamical eqilibrium at the boundary between gas and liquid with a turbulent ideal mixed bulk phase (both gas and liquid) and a laminar stationary boundary layer in the liquid phase. In the turbulent phase convective mass transport with neglectable concentration gradient dominates different to diffusive mass transfer in the laminar boundary layer [13].

Based on these assumptions, Lewis and Whitman (1924) introduced, the following description for the volumetric transport coefficient for different components.

$$k_L a_i = \frac{D_i}{\Delta x} \cdot \frac{A}{V} \qquad (2.23)$$

The coefficient depends on the diffusion coefficient of the specific gas, the thickness of the laminar liquid boundary layer (which is much thicker than the gaseous boundary layer) and the quotient of phase boundary layer area and the fluid volume, which is usually summarized as 'a', the specific gas-liquid phase boundary area [17]. If an independent film thickness is assumed, $k_L a_i$ only differs in the diffusion coefficient of the component i.

Following the gas transfer rate is proportional to the volumetric transport coefficient $k_L a$ and the driving force (2.24). The volumetric transport coefficient $k_L a$ describes the efficiency of the mass transport from gaseous to the liquid phase and depends mainly on the speed of the gas flow and the power input [13]. It also helps to compare different stirrer geometries and bioreactor designs and is also a valuable

tool for process optimization. On the other hand the volumetric uptake rate is definded as the cell specific amount of assimilated dissolved gas (2.25).

$$Transfer\ Rate = \frac{dc}{dt} = k_L a \cdot (c_g{}^* - c_g) \tag{2.24}$$

$$Uptake\ Rate = q_S \cdot c_X \tag{2.25}$$

2.4.1. Henry´s Law

Henry's law describes the proportion between the amount of dissolved gas to the partial pressure in the gas phase above the liquid at standard conditions (T_{Std}=298.15K) for a small concentration at the thermodynamical equilibrium.

$$H_i = \frac{c_i{}^*}{p_i} \tag{2.26}$$

A simple way to describe Henry's law as a function of temperature is:

$$H_{i,T} = H_{i,Std} \cdot exp\left(C_i \cdot \left(\frac{1}{T} - \frac{1}{T_{Std}} \right) \right) \tag{2.27}$$

$$C_i = \frac{-d\,ln\,H_i}{d\frac{1}{T}} = \frac{\Delta H_{sol}}{R} \tag{2.28}$$

Table 2.1.: Henry constants and temperature coefficients [54]

	$H_{i,Std}$	C_i
	[mmol/L ·bar]	$[K]$
O_2	1.28	1700
CO_2	33.55	2400
CO	0.93	1300
H_2	0.77	500

Figure 2.9 left shows the big differences in the Henry´s constants and therefore the gas solubilities must be respected to maintain a proper substrate supply.

This law provides the last piece to describe the transfer rates for the relevant gaseous
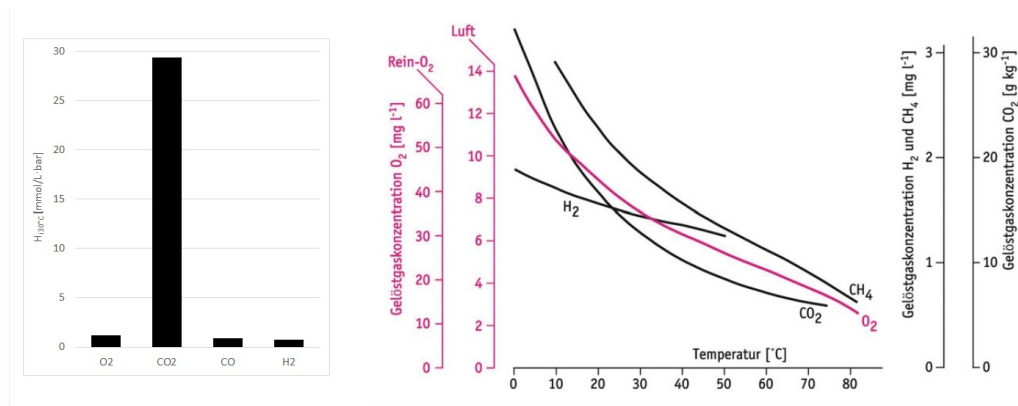
Figure 2.9.: Left: Comparison of Henry constants for utilized gases at 30 °C
Right: Temperature dependant solubility of biological relevant gases in water. Left axis- pure oxygen (oxygen partial pressure 1 bar) and air (oxygen partial pressure 0.21 bar), right-axis: pure methane, hydrogen and carbon dioxide (partial pressures 1 bar). Figure taken from [13]

substrates used in *A. woodii* cultivations.

$$HTR = k_L a_{H_2} \cdot (c_{H_2}{}^* - c_{H_2}) \tag{2.29}$$

$$CDTR = k_L a_{CO_2} \cdot (c_{CO_2}{}^* - c_{CO_2}) \tag{2.30}$$

2.5. Soft sensor

The combination of software-implemented models and hardware sensors is called a soft sensor [42]. This concept helps to 'measure' not directly available or only at high efforts and costs available signals. Furthermore calibration and validation procedures are minimized but consequently the sensitivity and accuracy suffers [13].
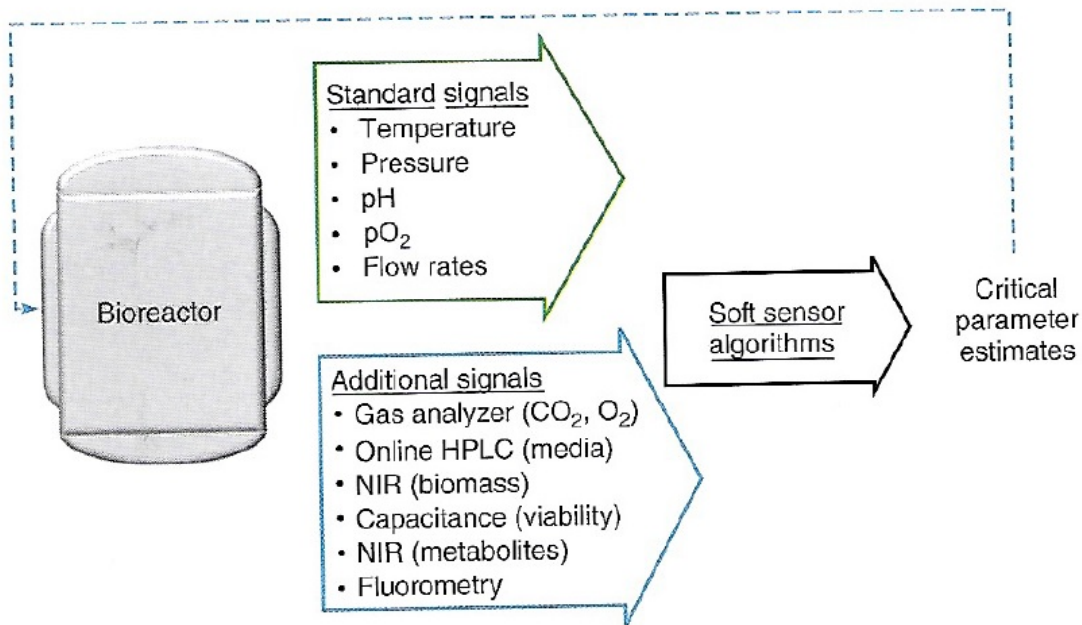
Figure 2.10.: Soft sensor concept. Figure taken from [42]

3. Material and Methods

3.1. *Acetobacterium woodii* strains

All cultivations and experiments in the scope of this work were carried out with the wild strain of *Acetobacterium woodii* (DSM 1030) obtained from the Deutsche Sammlung von Mikroorganismen und Zellkulturen, Braunschweig, Germany.

Cyro stocks were produced from an exponential growing cell culture (2x 50 mL). The cells were centrifuged, resuspended in fresh media (DSMZ 135) and mixed with glycerol to a final concentration of 10 v% glycerol and stored at -80 °C.

3.2. Anaerobic workplace

A. woodii is a representative of the strictly anaerobic microorganisms and therefore it is vital to ensure an oxygen free atmosphere and media during all cultivation procedures. Specific anaerobic working techniques, such as media and preculture preparation as well as cell harvest are described by Hungate and Macy [32].

The anaerobic workbench, as seen in figure 3.1, is a gas-tight PVC chamber with a material sluice (Toepfer Lab Systems, Göppingen) filled with gaseous nitrogen and 5 % hydrogen. Two catalytic fan boxes (COY Lab Products, Michigan) with palladium catalysts and a desiccant are present to generate a well mixed atmosphere and convert hydrogen and existing oxygen to water and therefore provide an oxygen free environment. For the transfer of material into the chamber, the sluice was evacuated and afterwards flushed with the mentioned gas mixture (nitrogen with 5 % hydrogen). This procedure was repeated at least three times to reduce the entering oxygen to a minimum (according to SOP A.2).
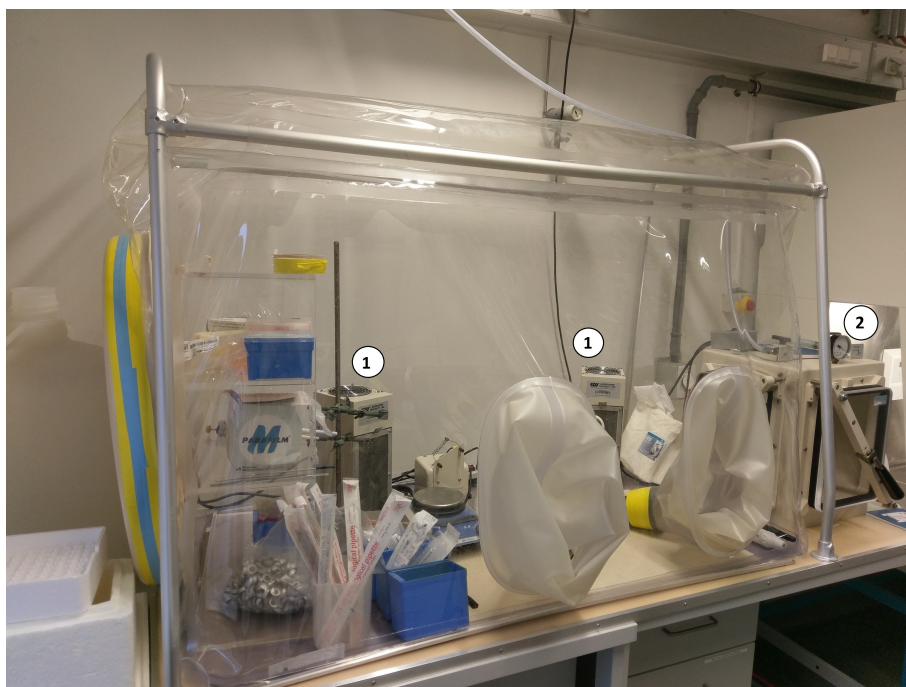
Figure 3.1.: Anaerobic chamber. (1) catalytic fan boxes. (2) material sluice.

3.3. Cultivations

3.3.1. Media preparation and composition

DSMZ 135

In the scope of this work a slightly modified media, based on the recommended media DSMZ 135 A.1 (from the Deutschen Stammsammlung von Mikroorganismen und Zellkulturen) for *A. woodii*, was mainly used for the experiments.

The final sodium concentration in the media was reduced to 50 mM Na^+ as Kantzow et.al.[36] demonstrated best growth and productivity for Na^+- concentration between 20 mmol and 250 mmol. Additionally severe inhibitions were shown for concentrations below 0.3 mmol and above 800 mmol.

The trace elements and yeast extract were doubled for optimal growth based on results of Demler et.al.[15]. For easier handling and due to no significant problems the sodium sulfide was omitted in bioreactor cultivations. All ingredients except bicarbonate, vitamins and cysteine were dissolved in distilled water, brought to the boil and cooled to room temperature under a 80 % H_2 and 20 % CO_2 gas

26

atmosphere. Then the bicarbonate was added and the media equilibrated under the same gas atmosphere to a pH around 7.4. Afterwards the media was filled in gas-tight serum bottles and autoclaved or directly sterilized in the bioreactor. Before useage sterile, anoxic stock solutions of cysteine, sodium sulfite and vitamins were added.

Table 3.1.: Compositions of complex media on basis of DSMZ 135 [A.1] for gas fermentation

Compound	Concentration	Unit
NH_4Cl	1.00	g/L
KH_2PO_4	0.33	g/L
K_2HPO_4	0.45	g/L
$MgSO_4$ x 7 H_2O	0.10	g/L
Trace element solution [A.2]	40	mL/L
Yeast extract	4.00	g/L
$NaHCO_3$	4.20	g/L
Vitamin solution [A.3]	20	mL/L
L-Cysteine-HCl x H_2O	0.50	g/L

Minimal media Heise/Reidlinger

This media recipe was taken from Heise et.al. [28]. All ingredients except selenite solution, vitamins, cysteine and trace elements were dissolved in distilled water and where made anaerobically through stirring for 30 min in the anaerobic chamber. Afterwards the media was filled into serum bottles and autoclaved. Before useage the sterile, anoxic stock solutions of selenite, cysteine, trace elements and vitamins were added.

Independent of the different media, anoxic and sterile fructose or glucose stocks were added for final concentrations of 10 g/L as a carbon source in hetero- and mixotrophic conditions.

Table 3.2.: Minimal media

Compound	Concentration	Unit
NH_4Cl	1.35	g/L
KH_2PO_4	0.2	g/L
$CaCl_2$ x 2 H_2O	0.11	g/L
$MgSO_4$ x 7 H_2O	1.45	g/L
KCl	0.50	mL/L
NaCl	1.16	g/L
$KHCO_3$	6.00	g/L
Selenite solution [A.5]	1.00	mL/L
Vitamin solution [A.3]	20	mL/L
L-Cysteine-HCl x H_2O	0.50	g/L
Trace element solution SL9 [A.4]	1	mL/L

3.3.2. Industrial flue gases

The gas compositions were focused around real applications and were therefore similarly chosen to two existing flue gas streams from industrial partners. Both gas compositions contain different amounts of different inhibitory components, namely CO, O_2 and CH_4 (see table 3.3). The applied gas mixtures, named VOEST and OMV, were mixed from pure gases due to the unavailability of real flue gases. For comparative purposes an idealized gas mixture was introduced with only N_2, CO_2 and 30 % H_2 (to ensure proper availability of hydrogen due to lower solubility).

Table 3.3.: Gas compositions in %

	VOEST	VOEST idealized	OMV	OMV idealized
N_2	46.6	47	75.2	58
CO_2	22.9	23	11.9	12
H_2	4.0	30	0	30
O_2	0	0	2.5	0
CO	25.4	0	0	0
H_2O	0	0	10.4	0
CH_4	1.0	0	0	0

3.3.3. Preculture and inoculum

In a 125 mL serum bottle 1 mL of thawed cryo stock was added to 50 mL of fresh media for cultivation. After three to four days it was transferred to further serum bottles to obtain a proper amount of biomass for inoculation. Serum bottles with volumes of 125 mL or 500 mL were used for precultures and inoculum.

Figure 3.2.: Serum bottles: left 500 mL, right 125 mL

The media (table 3.1) was first stirred in the anaerobic chamber to make it anaerobic. Afterwards the bottles were filled, sealed with a rubber septum and sterilized (121 °C, 20 min). The 125 mL bottles were filled with 50 mL of media and the 500 mL bottles were filled with 200 mL of media. After sterilization anoxic stocks of vitamins, cysteine and fructose or glucose ($10 \, gL^{-1}$) as a carbon source were mixed and stirred in the anaerobic atmosphere to reduce oxygen to a minimum (approx. 30 minutes) and added via sterile filtration and steril needles through the septum. Then, via a sterile filter and a needle, the headspace was evacuated and flushed at least three times with a gas mixture of 80 % H_2 and 20 % CO_2 and finally pressurized with 0.5 to 1.5 bar overpressure (according to SOP A.3).

The warmed bottles were inoculated with 1 mL (125 mL bottle) or 4 mL(500 mL bottle) of preculture. They were incubated at 30 °C at 200 rpm in an Infors HT lab shaker (Infors AG, Bottmingen, Switzerland).

In the following step the cultivation broth was centrifuged (4000 g at 25 °C, 30 min) and the pellet resuspended with sterile anaerobic deionized water and centrifuged again. Then the pellet was resuspended in a small amount (as little as possible)
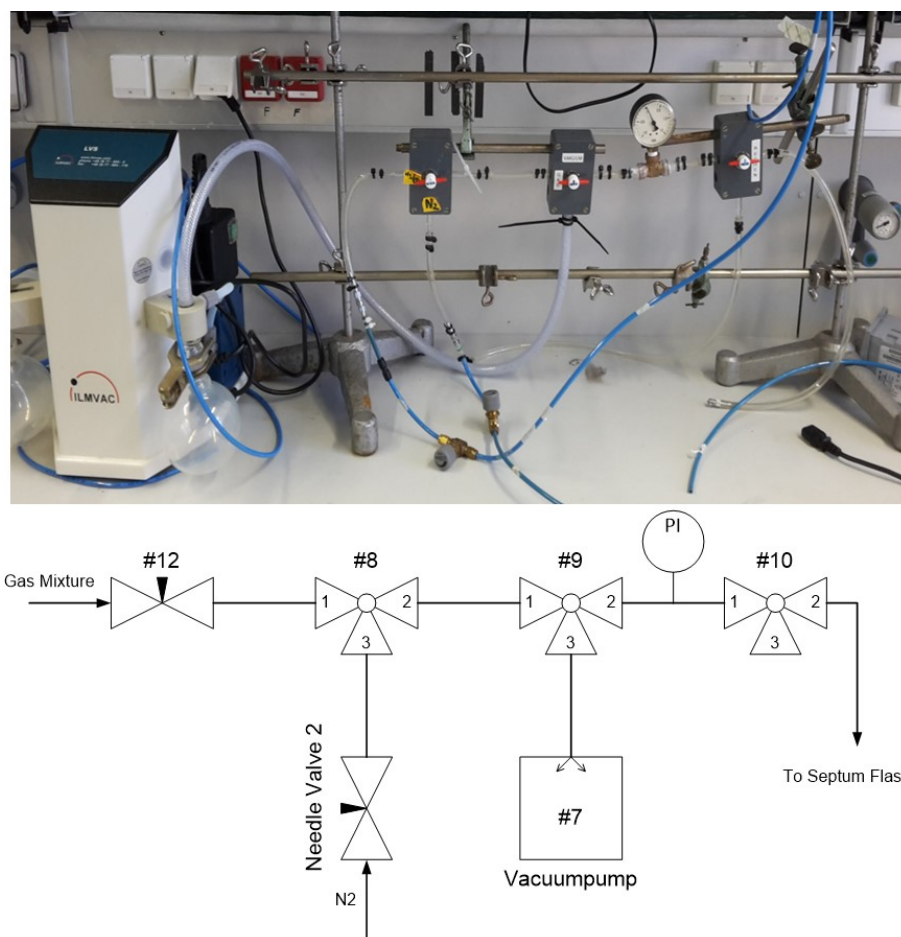
Figure 3.3.: Top: gas filling station for serum bottle; bottom: scheme of gas filling station.

of water and transfered into sterile syringes for inoculation of the reactors. It is essential to guarantee an oxygen free atmosphere throughout all those steps.

3.3.4. Serum bottle experiments

Serum bottles (125 mL) were used for hetero-, mixo- and autotrophic preliminary tests. The bottles were filled with anaerobic media (depending on the experiment) in the anaerobic chamber, sealed with a rubber septum and sterilized (121 °C, 20 min). After sterilization, sterile, anoxic stocks of all components which were sensitive to heat (e.g. vitamins, cysteine) were added with steril syringes. Then, via a sterile filter and a needle, the headspace was evacuated and flushed three times with the relevant gas mixtures and pressurized with 1.0 bar overpressure. The warmed flasks were inoculated with 1 mL of preculture. They were incubated at 30 °C at 200 rpm

in an Infors HT lab shaker (Infors AG, Bottmingen, Switzerland). All experiments were carried out with at least two flasks per condition tested. For sampling, 1 mL of broth was withdrawn with a sterile syringe.

3.3.5. Cultivations in lab fermenter

Fermenter F7

All cultivations were conducted in a 10 L double jacket (heating/cooling) stainless steel laboratory reactor (Biostat C+, Sartorius, Göttingen). Temperature was controlled to 30 °C. The gas mixture was provided with 3 MFCs (Brooks, Dresden, Germany) for CO_2, H_2 and air and added through a 0.2 μm filter and dispensed by two sintered spargers with a pore size of 20 μm. The culture broth was stirred with 3 disc-mounted flat-blade turbine stirrers (20-1500 rpm). The pH value and redox potential were monitored with electrochemical electrodes (Mettler Toledo, Ohio, USA) and pH was controlled by adding 5 M KOH via the integrated pump module of the bioreactor. NaOH should be avoided for pH control to maintain the ideal range for the Na^+-concentration.

The feed for continous cultivations was supplied by a peristaltic pump (Preciflow Lambda, Zürich, Switzerland) and the harvest was withdrawn by a digital peristaltic pump (Ismatec, Wertheim, Germany). Feed, harvest and base bottles were linked to the bioreactor setup with silicon tubings and bajonette connectors. Feed and base were added from the top and the harvest was withdrawn from the submerse sampling valve of the bioreactor and were gravimetrically quantified with balances (Sartorius, Göttingen, Germany) to record the weight changes.

Process parameters were adjusted and recorded via the process information management system (PIMS, Lucullus, Securecell, Switzerland) or the in-build touch screen control panel.
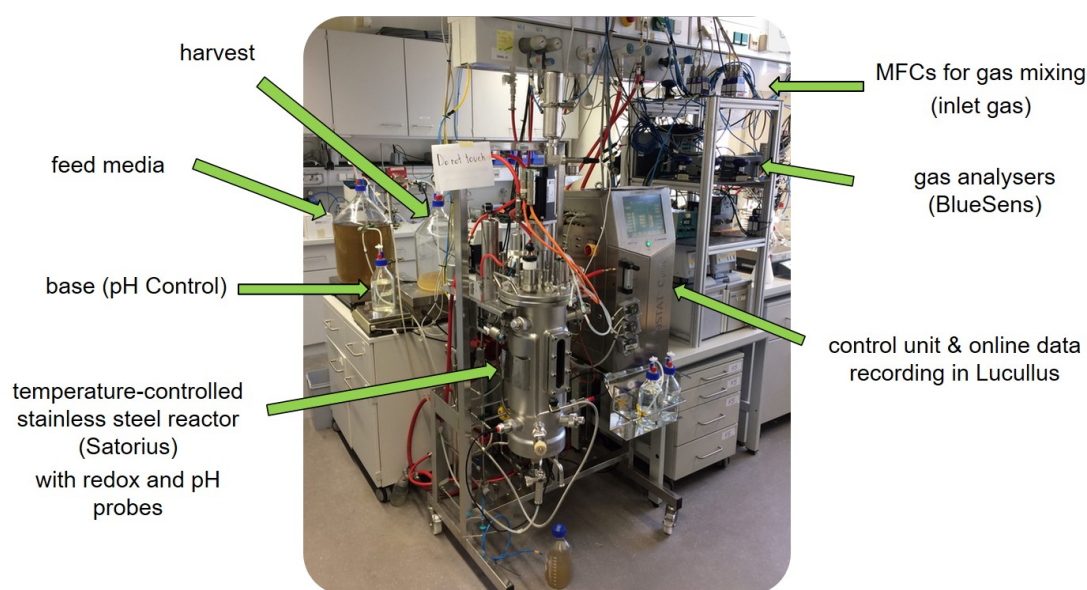
Figure 3.4.: Bioreactor Setup Sartorius Biostat C+ 10 L

Fermenter F11

Fermenter F11 is a 1 L double jacket (only heating) glas laboratory reactor (Applikon, Holland) and was planned for a long term continuous cultivation to evaluate gas switching procedures. Temperature was set to 30 °C. The gas mixture was provided with 3 MFCs (Brooks, Dresden, Germany) for CO_2, H_2 and air and added through a 0.2 μm sterile single use filter and dispensed by a pressure immersion tube with small holes. The culture broth was stirred with 3 disc-mounted flat-blade turbine stirrers (20-1500 rpm). The pH value was monitored with an electrochemical electrode (Mettler Toledo, Ohio, USA) and was controlled by adding 1 M KOH via a digital peristaltic pump (Ismatec, Wertheim, Germany).

The feed for continuous cultivations was supplied by a peristaltic pump (Preciflow Lambda, Zürich, Switzerland) and the harvest was withdrawn by a digital peristaltic pump (Ismatec, Wertheim, Germany). Feed, harvest and base bottles were linked to the bioreactor setup with silicon tubings and bajonette connectors. Feed and base were added from the top and the harvest was withdrawn from the submerse tube of the bioreactor and were gravimetrically quantified with balances (Sartorius, Göttingen, Germany) to record the weight changes.

Process parameters were adjusted and recorded via the process information man-

agement system (Lucullus PIMS, Securecell, Switzerland).
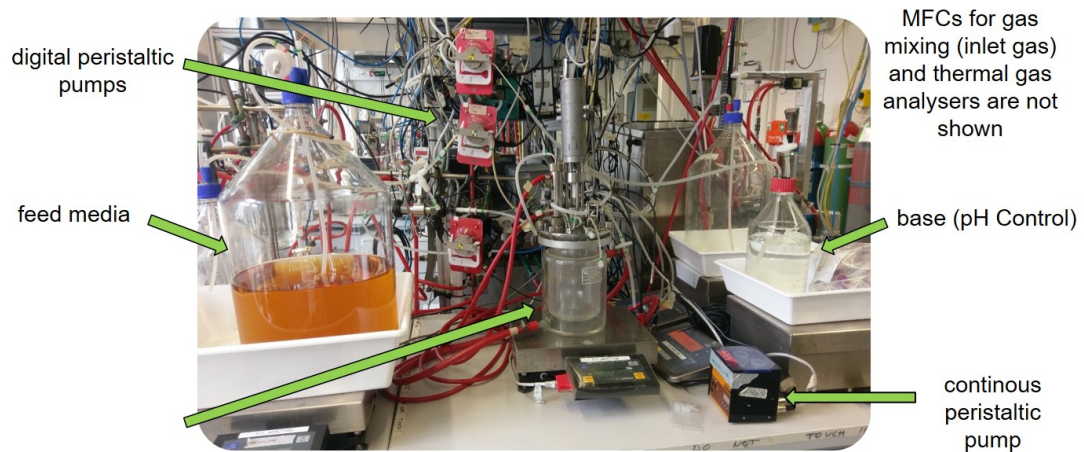
Figure 3.5.: Bioreactor Setup Applikon 1 L

3.3.6. Lucullus Process Information Management System (LPIMS)

LPIMS (Securecell, Switzerland) unifies the core competences (planning, preparation, execution, evaluation) of process development in one system. It provides an easy-to-handle user interface for reactors and devices as well as data recording and process control. In the scope of this work it was mainly utilized for set-point specification (gassing rates, agitator speed, temperature, etc.), visualization of online data during fermentations, control of parameters (pH, inflow and outflow rates for chemostat fermentations) and data export for further calculations.

In addition, the provided Online Tool of LPIMS was used to develop online calculators for important physiological (e.g. gas uptake rates and base rate) and process relevant (e.g. gas transfer rates) parameters. In addition, the applicability of a soft sensor setup for biomass and metabolites throughout the cultivations was analysed and tested.

These calculators were elaborated to evaluate trends during cultivations. This could further help to conduct experiments in a different way as well as getting closer to an industrial setting with measurable, predictable and controllable set-points, with respects to those trends.

3.4. Analytical methods

3.4.1. Biomass Dry Weight and OD$_{600}$

For determination of the cell dry weight and the following correlation with the optical density at 600 nm was determined gravimetrically in triplicate of the cultivation broth. 6 mL of cell suspension were centrifuged (Sigma 3-18KS with Sigma 11133 rotor and four 13104 beakers, Osterode am Harz, Germany) at 14000 rpm, 4 °C for 15 minutes in pre weighted glass tubes. 2 mL of the cleared liquid was used for HPLC analytics and the remaining supernatant was discarded. The cell pellet was washed with 3 mL of distilled water, centrifuged again and the washing liquid discarded. After a minimum of 72 hours at 105 °C in the drying chamber the cell dry weight was measured.

The optical density of the cultivation broth was measured with a photometer (Genesys 20, Thermo Fisher Scientific, Massachusetts, USA) at a wavelength of 600 nm. The dilution of the sample was chosen to fit the linear range of 0.2 to 0.7 absorption units of the device. The cell dry weight in g/L can be correlated with the following equation.

$$CDW = 0.413 \cdot OD_{600} - 0.095 \tag{3.1}$$

The big advantage of that measurement is the at-line availability of the data compared to the cell dry weight determination.
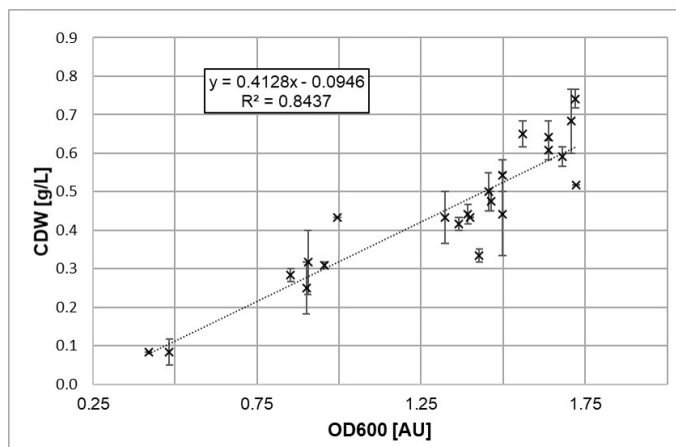
Figure 3.6.: Linear regression for CDW and OD$_{600}$ relation

As a further improvement an online turbidity probe 316L (Fogale nanotech, Nimes, France) with a measurement at a wavelength of 880nm was applied.

3.4.2. HPLC analytics

The screening of metabolites in the cultivation broth was carried out with an HPLC (Agilent Technologies, Santa Clara, USA). The set up consisted of a degasser unit, a quaternary pump, an autosampler with a tray for 100 vials, a thermostat, a column compartment unit, a refractive index detector and a diode array detector. The utilized column was an Aminex HPX-87H (Bio-Rad Laboratories Inc., Hercules, California, USA) which is suitable for the analysis of carbohydrates in solution with carboxylic acids, volatile fatty acids, short-chain fatty acids, alcohols, ketones, and neutral metabolites. A method with 0.6 mL/min flow rate, column temperature of 60 °C and a run time of 30 minutes was used.

The sample was, if necessary, melted and centrifuged (Sigma 3-18KS, rotor Sigma 12349, Osterode am Harz, Germany) again. 450 μL of sample and 50 μL of 40 mM sulfuric acid were filled into vials and sealed. The RID signal was used to evaluate the metabolite concentrations. As a mobile phase 4 mM sulphuric acid prepared with MQ water and a spatula tip of NaN_3 was utilized.

3.4.3. Offgas analytics

The bioreactor setups were equipped with BlueSens gas sensors (BlueSens, Herten, Germany) to measure the offgas composition online.

Figure 3.7.: Online offgas sensor, BlueSens

The CO_2 sensor is fitted with an infra-red radiation source and a detector. The absorption of the radiation from CO_2 molecules is measured. The H_2 sensor is a thermal sensor which measures the difference between thermal conductivity of H_2 and a reference gas. The values were corrected in accordance to the manufacturers instructions.

3.5. k_La determination

The volumetric transport coefficient was determined with the so called „dynamic method". The diluted oxygen concentration was measured with a VisiFerm DO 120 probe (Hamilton, Nevada, USA).

Due to possible positive and negative effects of media components, it is recommended to evaluate k_La under real cultivation conditions to ensure conditions comparable to cultivations [13].
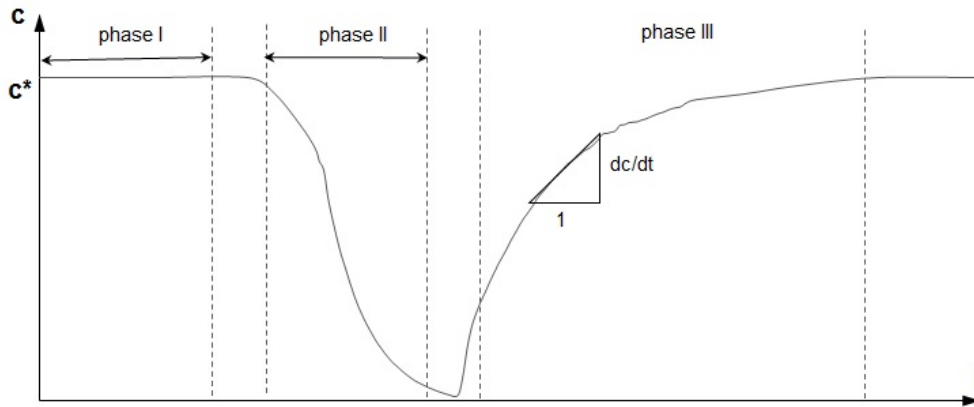
Figure 3.8.: Methodology for k_La determination with the dynamic method

In phase I the reactor is in a stationary state. c* is the saturated oxygen concentration in the liquid phase. The air supply is changed to pure nitrogen and this leads to phase II and the reduction of oxygen in the reactor until a low value or zero is reached. In phase III the gassing is changed to air again and the dissolved oxygen concentration increases back to c*.

The obtained slope dc/dt or the oxygen uptake rate, the equilibrium concentration from equation (2.26) can be combined with (2.24). A linear regression with the

measured values of dc/dt over (c*-c) leads to the volumetric transport coefficient for oxygen. Equation (2.23) determines $k_L a$ for different gases.

The determination of the volumetric transport coefficients ($k_L a$-values) for the fermenter F7 was carried out with water, at the standard cultivation temperature of 30 °C for *A. woodii*. After calibration of the dissolved oxygen probe, all normalized set-points were measured in random order (see table 4.1). The set-points are normalized between -1 and +1 to enable an easier calculation later. The set-point area was based on previously conducted experiments and on published data [36], [15].

Table 3.4.: Design of Experiment normalized set-points

	Agitator speed [min^{-1}]	Gassing [L/min]
-1	900	0.25
0	1200	2.5
+1	1500	4.75

3.6. Colony-PCR

The screening for cellular impurities within cultivations and inoculation was made with a combination of Colony-PCR and simply gram staining.

For gram staining a small amount of cells were distributed on glas carrier plates in a sterile environment (LaminarFlow). Afterwards it was treated with a Gram kit (Carl Roth GmbH, Karlsruhe, Germany) strictly following the user guide instructions and then a microscopic screening was done.

For the Colony-PCR, 50 μL of the solution below (table 3.5) was prepared for each colony (either from petri dishes or serum bottle cultures) and each primer. A small amount of centrifuged cell pellet or scrapped off colony was added to the master mix. DNA polymerase was added to the reaction mixture and then everything was mixed properly in small eppis and filled into the thermal cycler (S1000, Bio-Rad Laboratories Inc., Hercules, California, USA). The cycle program settings were 98 °C for lysis, 61 °C annealing temperatur and 80 s elongation time for 37 cycles.

Table 3.5.: Mixture for Colony-PCR, Prepared cryo stock

Compound	Amount [μL]
TRIS 10mM	33.5
Q5 Reaction buffer	10
Primer Forward	2.5
Primer Backward	2.5
dNTPs	1
Q5 Polymerase	0.5

After completion an agarose gel for the gel electrophoresis (PowerPack Basic, Bio-Rad Laboratories Inc., Hercules, California, USA) was loaded with 6 μL GeneRuler and 10 μL of PCR solution. The settings were 120 V for 60 min.

The identification of *A. woodii* was made with a fdhF1 fw/rev primer to yield a product of 2200 bp and metE fw/rev primer to yield a product of 2289 bp (both primer sets: IDT DNA, Coralville, Iowa, USA). The gene fdhF1 is exclusively existent in *A. woodii* and therefore non existent in *E. coli*. The gene metE is exclusively existent in *E. coli* and therefore non existent in *A. woodii*. Hence no PCR product should be observable for the combination fdhF1 with *E. coli* and metE with *A. woodii*. For each primer pair a negative control without template was made.

4. Results and discussion

4.1. Mass transfer

The volumetric transport coefficient $k_L a$ has a major importance for gas-liquid mass transfer in the cultivation broth. Most physiological relevant gases are poorly soluble in liquids, as described in section 2.4.1. The Henry constant of hydrogen is approximately 30 times lower in comparison to carbon dioxide (see figure 2.9), hence a hydrogen limitation is possible.

Therefore results according the gas/liquid mass transfer are necessary for the physiological important gas components CO_2 and H_2.

A first failed DoE led to a driving-force limited experiment (data not shown), and thus the method was adapted slightly. Due to the big head-space above the liquid level, an undefined gaseous atmosphere was present. In consequence, non-plausible results were obtained. A ten minutes flushing of the head-space atmosphere, without stirring, solved this issue.

As described in 3.5 the $k_L a$ value for oxygen can be derived from the measured dissolved oxygen data. There was no necessity for any smoothing of the observed raw data.

An increase of the agitator speed from 900 to 1500 rpm at the highest gassing rate increased the $k_L a_{O_2}$ from 255 h^{-1} to 321 h^{-1}. For the lowest gassing rate of 0.05 vvm an increase from 222 h^{-1} to 298 h^{-1} was obtained.

Table 4.1.: Results and Design of Experiment table for $k_L a_{O_2}$ determination in fermenter F7

Experiment	$k_L a_{O_2}$ [h^{-1}]	Agitator speed	Gassing
1	305	0	0
2	321	+1	+1
3	298	+1	-1
4	301	0	0
5	255	-1	+1
6	222	-1	-1
7	304	0	0

In order to assess the influences on the final figure (calculated values for k$_L$a) for the decisive parameters, agitator speed and gassing rate, the following equation (4.1) is introduced:

$$\bar{y} = \bar{b} \cdot \bar{F} \tag{4.1}$$

$\bar{y}$ is a vector and represents the assessed value, $\bar{F}$ is a matrix including the normalized parameters and $\bar{b}$ is a model parameter vector to evaluate the specific influences. The calculation of $\bar{b}$ was done in RStudio with a linear model fit over a regression.

As shown in figure 4.2 both parameters, agitator speed and gassing rate, have a positive influence on the assessed value $\bar{y}$, the volumetric transport coefficient. The standard error bars indicate the significance of the parameters. Therefore only the agitator speed has a significant positive influence on the k$_L$a but the influence of the gassing rate is not significantly. This leads to a reduced linear model, with just one parameter (agitator speed) left.

The equation (2.23) and the diffusion coefficients for oxygen ($2.1 \cdot 10^{-9} m^2/s$), hydrogen ($3.901 \cdot 10^{-9} m^2/s$) and carbon dioxide ($2.32 \cdot 10^{-9} m^2/s$) [15] led to the final k$_L$a [h^{-1}] value models.

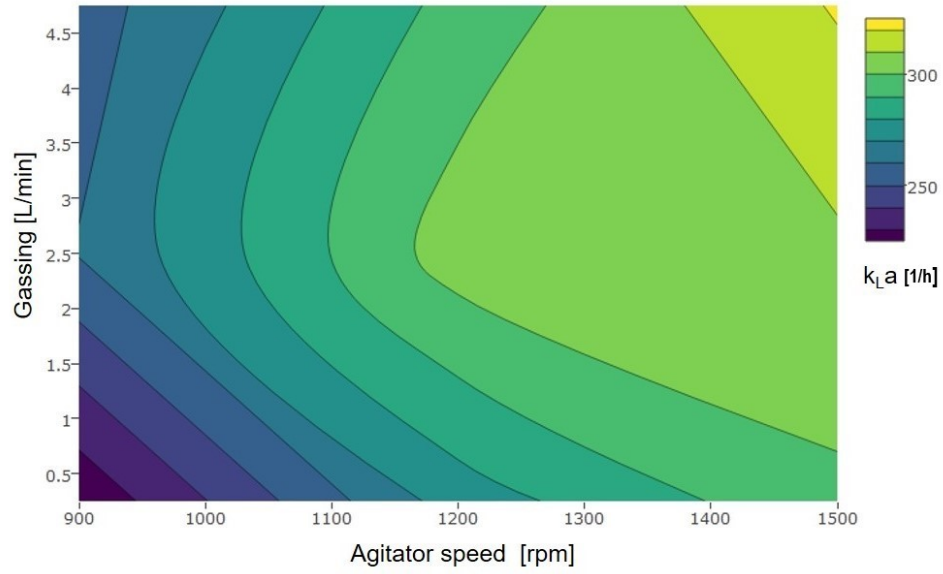Figure 4.1.: Contour plot of the multi-linear regression model for the k_La
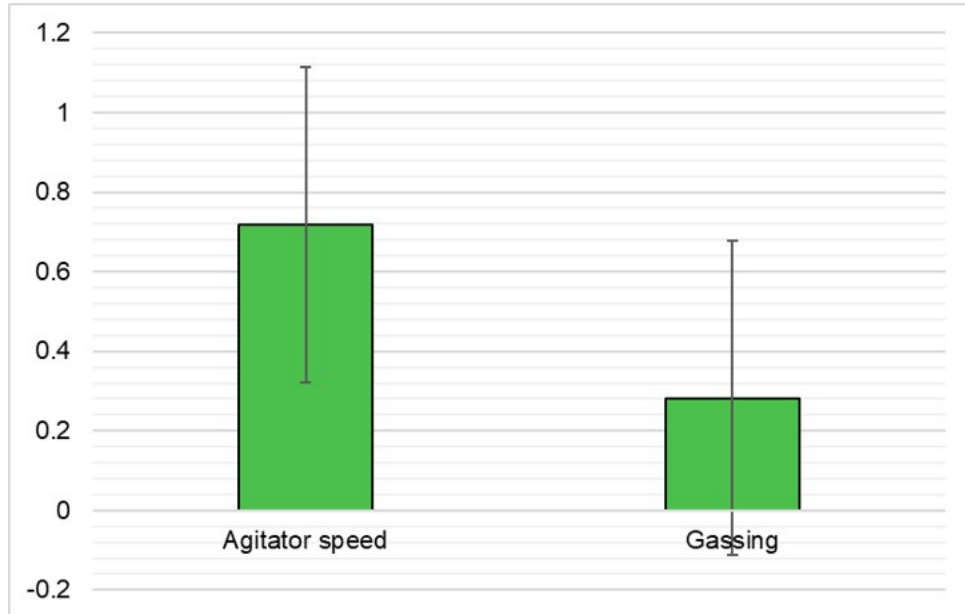

Figure 4.2.: Box plot of the fitted model parameter vector $\bar{b}$

$$k_{La\,O_2} = 0.1183 \cdot Agitator\ speed\,[min^{-1}] + 144.7 \tag{4.2}$$

$$k_{La\,CO_2} = 0.1307 \cdot Agitator\ speed\,[min^{-1}] + 159.9 \tag{4.3}$$

$$k_{La\,H_2} = 0.2198 \cdot Agitator\ speed\,[min^{-1}] + 268.8 \tag{4.4}$$

$$model\ fit\ R^2 = 70\,\% \tag{4.5}$$

The volumetric transport coefficients for the standard cultivation conditions (1200 rpm, 0.1 vvm) are therefore $k_L a_{CO_2} = 317\,h^{-1}$ and $k_L a_{H_2} = 533\,h^{-1}$

4.1.1. Discussion

The positive effects of both parameters were to be expected and can be explained by the two-film model. The specific boundary area 'a' has a positive influence on the volumetric transfer coefficient, as seen in equation (2.23). Higher agitator speeds result in an improved mixing regime and higher shear forces. For this reason the average gas residence time, the amount of bubbles and the average surface area per bubble increase. Higher gassing rates also cause an increase in the amount of bubbles and the average surface area per bubble, but can reduce the average residence time and consequently the equilibrium can not be reached properly. This may be the cause of the non significant influence. In the contour plot of the fitted multi-linear regression model this phenomenon can also be observed (figure 4.1). For gassing rates above 2.5 L/min a distinct non-linearity is noticeable.

The initial linear model including both parameters had a goodness of fit, R^2, of 78 % which already indicates non-linearities. The simplified model with just the agitator speed had a final goodness of fit of 70 % which reveals that there are still non-linearities, presumably due to saturation effects. In addition, the submersed sparger is fitted with a sintered sparger (pore size 20 μm) and leads to the assumption of a uniform bubble size distribution from the sparger. The experiment was carried out with water without any additives (e.g. Antifoam), but due to the small uniform bubble size, influences of additives are possibly negligible. This reduces the possible influences on the residence time which may have caused these non-linearities throughout the experiment.

The final fitted model can be used for estimation and checking of the mass transfer performance, but as the R^2 value is relatively low this should not be used for any control procedures.

Due to the demonstrated performance of fermenter F7 regarding mass transfer, the

reactor design was not considered and the gassing rate, agitator speed, headspace pressure and hydrogen partial pressure remain as possible adjustments to improve the mass transfer performance.

The intensification of stirring was rejected due to the high agitator speed of already 1200 rpm and to avoid potential shear stress of *A. woodii*.

An increase of the headspace pressure would increase the driving force and therefore the HTR. This could help to improve the availability of hydrogen for the cells and an increase of the HUR is feasible. Kantzow [36] showed that an increase in head-pressure from 1.0 bar to 3.5 bar had negative effects on acetate formation (-22 %) and growth but increased the formate formation eightfold.

Higher gassing rates would also increase the driving force and therefore the HTR, but would also lead to higher remaining CO_2 concentration in the offgas. This would either be in contradiction with the desire to produce an almost carbon free offgas or require a gas circulation system for carbon sparse offgas.

Thereby the last remaining possibility for better mass transfer is an increase in the hydrogen partial pressure at ambient pressure. Due to the fact that the overall process concept would involve hydrogen from renewable resources and because the hydrogen separation technologies, for possible gas recycling, are advanced [31], an elevated hydrogen partial pressure might be the most feasible solution.

4.2. Examination of process modes and ideal gas compositions in lab fermenter

Several cultivations were carried out to evaluate important physiological parameters and furthermore to verify already published results.

The first experiments by Balch et.al.[3] resulted in small acetate concentrations and productivities. Big efforts on media development, process improvements and mass transfer by Kantzow et.al.[34],[36] led to the best results for an autotrophic cultivation on complex media for *A. woodii* published so far.

The highest reached acetate titer was 59.2 g/L in a STR (0.5 vvm; 40 % H_2, 16.7 % CO_2; 30 °C; 1200 rpm) resulting in a reaction rate $r_{acetate}$ of 18.7 g/L d and a biomass specific reaction rate $q_{acetate}$ of 6.93 g/g d. Furthermore peaking CDUR of 0.07 mol/L h and HUR of 0.125 mol/L h with a decrease to CDUR = 0.02 mol/L h and HUR = 0.045 mol/L h for constant biomass were measured. The highest achieved volumetric reaction rate or time-space-yield was obtained by a submerged membrane cell retention system in a CSTR with 147.8 g/L d [34].

Cultivation results for CSTR and submerged membrane CSTR cultivations (both 0.5 vvm; 60 % H_2, 25 % CO_2; 30 °C; 1200 rpm) are summarized in the following table 4.2:

Table 4.2.: Chemostat results from Kantzow et.al. [36]

	CSTR	submerged membrane CSTR
D [1/h]	0.035	0.350
$r_{acetate}$ [g/L d]	18.2	147.8
$q_{acetate}$ [g/g d]	16.55	13.69

Batch cultivation with stoichiometric gas ratio

This batch cultivation with an idealized gas mixture with 23 % CO_2 and 46 % H_2 (stoichiometric gas ratio according to equation (2.2)) was carried out to validate and compare published results for gas uptake rates, growth rates and productivities. Furthermore this cultivation was used as a comparison throughout all different cul-

Table 4.3.: Fixed setpoints for all cultivations

Parameter	Setpoint
pH	7.0
temperature	30 °C
gassing rate	0.1 vvm
pressure	1.0 bar
agitator speed	1200 rpm
V_R	5L

tivations in fermenter F7.

After 64.5 h of process time the N_2 gas cylinder unfortunately was empty and therefore the gas changed to 33 % CO_2 and 67 % H_2. These following results were not considered. In addition to that the standard cell dry weight determination failed for this experiment, so the biomass was estimated with the at-line optical density OD_{600} measurement (equation (3.6)).

The highest reached acetate concentration was 14.2 g/L at the end. A constant increase of formate to 0.73 g/L was observable, but was then subsequently consumed with the increased carbon dioxide and hydrogen concentration.

The hydrogen transfer rate for these conditions was estimated with equation 4.4 to 0.033 mol/L h. In contrast to that the average hydrogen uptake rate was in the same range with 0.039 mol/L h. A carbon dioxide uptake rate of 0.019 mol/L h led to an almost stoichiometric yield Y_{H_2/CO_2} of 2.05. The uptake rates indicate a constant increase over the first 64 h of cultivation which is probably caused by increased biomass.

Furthermore the acetate to hydrogen yield is 73 % and the acetate to carbon dioxide yield is 84 % of the theoretically possible yields. A maximum growth rate μ_{max} of 1.08 d^{-1} was observed. For this cultivation a volumetric reaction rate $r_{acetate}$ of 8.13 g/L d and a productivity $q_{acetate}$ of 13.2 g/g d was achieved.

The carbon balance with 87.9 % and the degree of reduction balance with 86.2 % did not sum up perfectly.
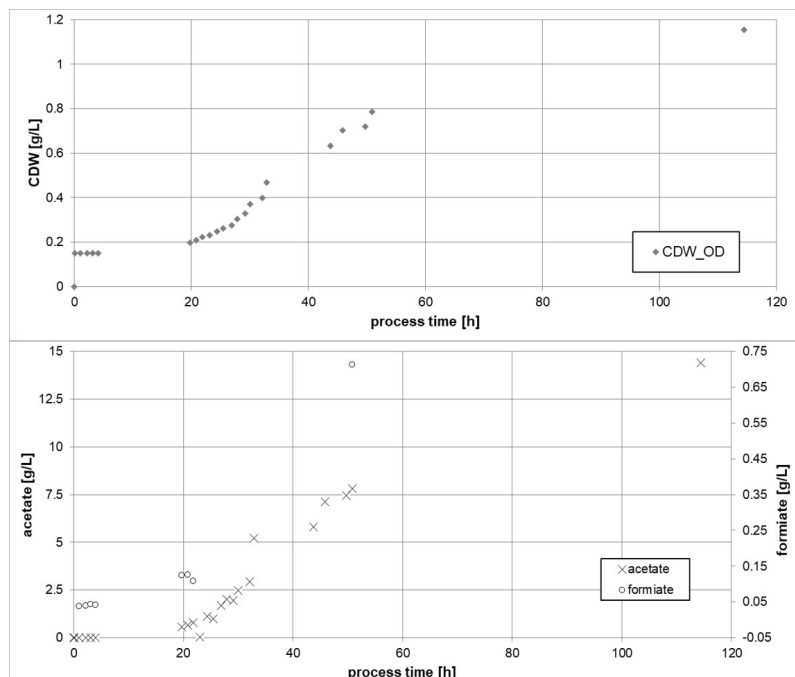
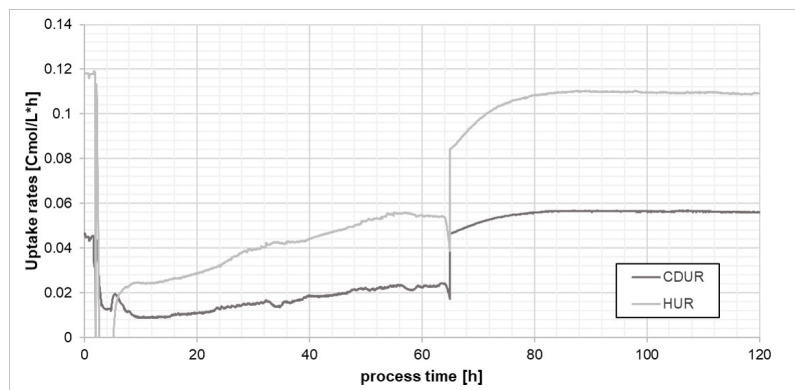Figure 4.3.: Cell dry weight and product concentrations over time

Figure 4.4.: Trends for the uptake rates of hydrogen and carbon dioxide

Batch cultivation with changing gas composition

In this experiment the gas composition was changed throughout a batch cultivation. The initial growth to a steady biomass concentration and further batch cultivation until 115 h of process time was carried out with an idealized gas mixture with 30 % CO_2 and 43 % H_2 (experiment B). After 115 h of process time the gas mixture was changed to 30 % CO_2 and 23 % H_2 (experiment C). The reduction of the hydrogen concentration throughout the fermentation should help to evaluate effects of gas changes and to identify resulting system limitations.

The highest reached acetate concentration was 24.3 g/L at the end. A constant increase of formate to 0.2 g/L was observable. The steady state biomass concentration was around 1 g/L.

The hydrogen transfer rate for the first conditions was estimated with equation 4.4 to 0.034 mol/L h and 0.025 mol/L h for the second gas composition.

The reduction of the hydrogen concentration changed the average hydrogen uptake rate from 0.035 to 0.014 mol/L h and the carbon dioxide uptake rate from 0.025 to 0.005 mol/L h. Additionally the uptake rate trends are very noisy. The uptake rates indicate a step increase in the inital growing phase and a constant decrease until the gas composition change at 115 h process time.

The growth rate μ was minorly affected by the gas switching procedure with a change from 1.06 to 0.94 d^{-1}.

In contrast, the volumetric reaction rate $r_{acetate}$ decreased by 47 % from 5.19 to 2.76 g/L d. The productivity $q_{acetate}$ was not badly affected and changed by 19 % from 7.26 to 5.88 g/g d.

The carbon and degree of reduction balance still did not sum up perfectly but were close to 90 %.
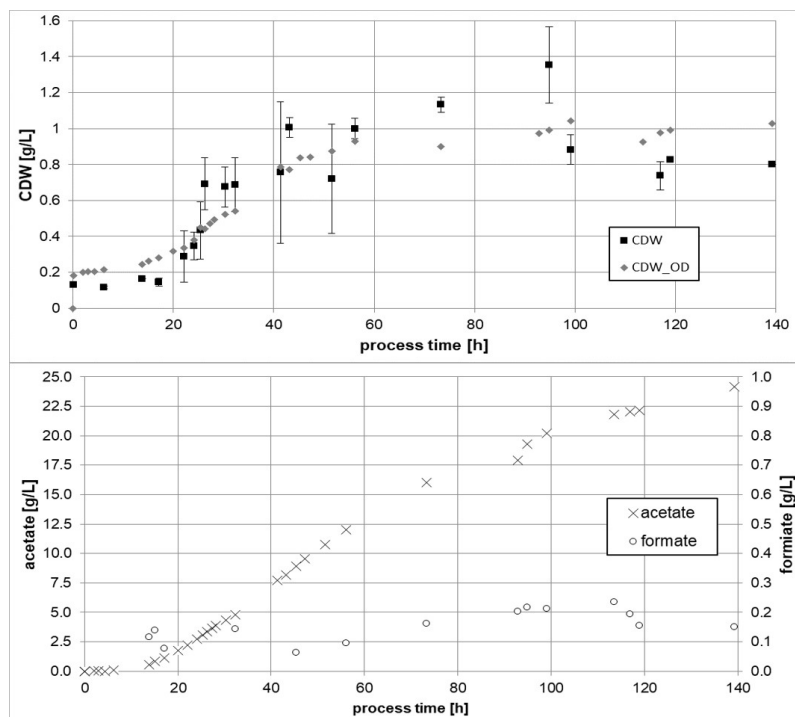
Figure 4.5.: Cell dry weight and product concentrations over time for experiments B and C
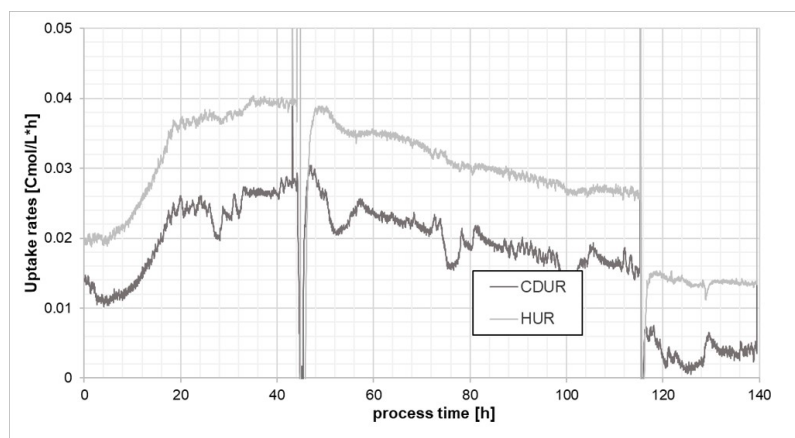

Figure 4.6.: Trends for the uptake rates of hydrogen and carbon for experiments B and C

Continuous cultivation with changing gas composition

A continuous cultivation with changing gas compositions was carried out to evaluate the influences of gas composition changes in a chemostat cultivation.

A batch cultivation led to a proper initial biomass concentration for the following continuous cultivation. These experiments were executed with the idealized industrial gas compositions (see table 3.3).

For the initial growth and the first chemostat phase the OMV idealized gas mixture (12 % CO_2, 30 % H_2) was applied (experiment D).

After 75 h of process time a constant feed with the dilution rate D = 0.023 h^{-1} (=2/3 μ_{max}) was started (experiment E). A digital peristaltic pump ensured a constant reactor weight (between $\pm$ 20 g) by withdrawing cultivation broth.

Three volume changes had been performed with continuous sampling before the gas mixture was switched to the idealized VOEST composition (table 3.3) gas mixture (23 % CO_2, 30 % H_2) at 350 h process time (experiment F). 1.27 volume changes were accomplished with this gas mixture.

Instead of autoclaving the media, prior to fermentation in the reactor and transferring it sterilely into a sterile bottle, the media was prepared in the reactor and transferred and autoclaved as fast as possible inside the 20 L feed media bottle in a big laboratory autoclave (Systec GmbH). This was necessary to maintain a sterile feed over the long cultivation duration of 400 h.

The steady state acetate concentration was constant and around 8.5 g/L for both gas mixtures. An increase of formate to 0.09 g/L during the lag phase was observable. The steady state biomass concentration was around 0.5 g/L.

The hydrogen transfer rate was constant and estimated with equation 4.4 to 0.013 mol/L h.

The feed start had no effect on either the hydrogen uptake rate of 0.012 mol/L h nor the average carbon dioxide uptake rate of 0.0065 mol/L h. The uptake rates indicate a step increase in the initial growing phase and have the same trend as the

biomass. Additionally the uptake rate trends are very noisy.

After the gas mixture change, a CDUR of 0.024 mol/L h exceeded the HUR with 0.02 mol/L h and therefore the yield Y_{H_2/CO_2} dropped below one (to satisfy the stoichiometry, a ratio of two would be necessary). A potential saturation effect of the cultivation broth could be the reason for this phenomenon but an additional evaluation is needed.

Due to the constant dilution rate, the growth rate μ was also constant with 0.551 d^{-1} throughout the gas composition change.

The volumetric reaction rate $r_{acetate}$ ranged between 2.98 and 3.19 g/L d. In contrast, the productivity $q_{acetate}$ ranged between 6.03 and 7.90 g/g d.

The carbon and degree of reduction balance did sum up properly with over 90 % for all three experiments.
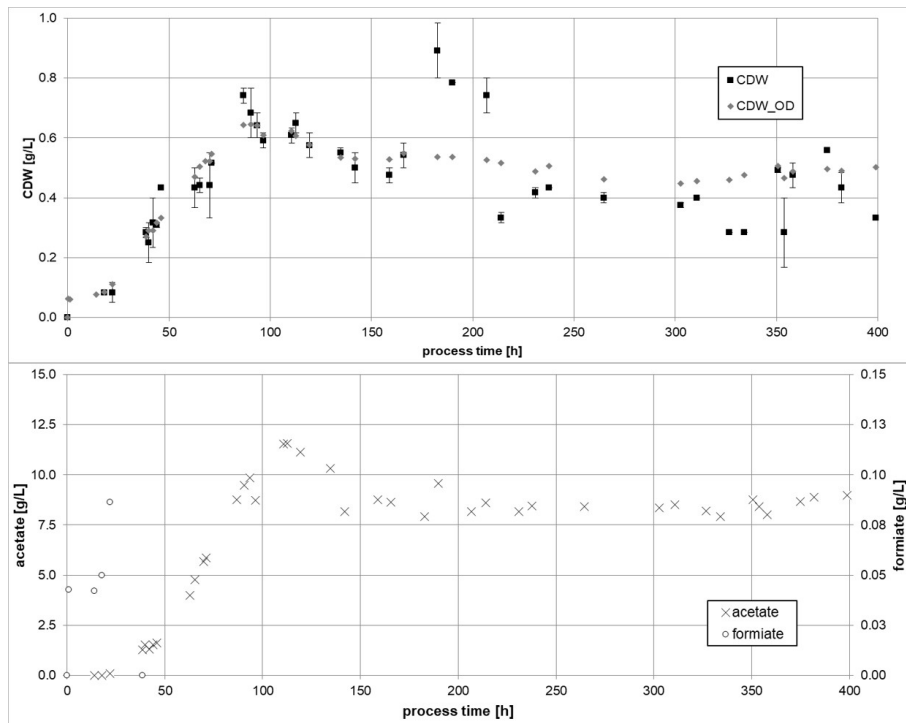

Figure 4.7.: Cell dry weight and product concentrations over time for experiments D, E and F
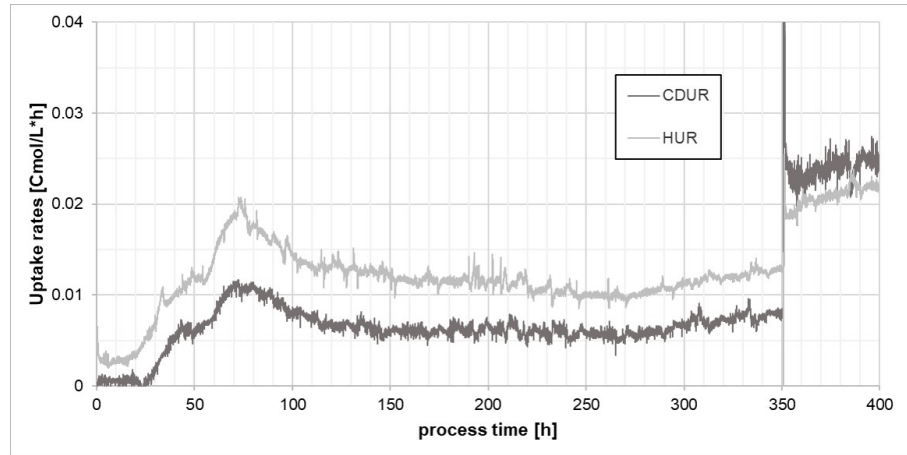
Figure 4.8.: Trends for the uptake rates of hydrogen and carbon dioxide for experiments D, E and F

Table 4.4.: Summarized results for all cultivations

	Carbon balance [%]	DoR balance [%]	$r_{acetate}$ [g/Ld]	$q_{acetate}$ [g/gd]	μ [1/d]
A	87.9	86.2	8.125	13.200	1.080
B	87.8	88.9	5.189	7.260	1.056
C	85.4	84.7	2.755	5.884	0.936
D	91.8	93.0	3.193	7.899	0.826
E	92.5	94.1	3.112	6.027	0.551
F	91.0	103.9	2.982	7.157	0.551

Table 4.5.: Summarized gas related results for all cultivations

	$\overline{HUR}$ $[mol/Lh]$	$\overline{CDUR}$ $[mol/Lh]$	$Y_{\frac{acetate}{CO_2}}$ $\left[\frac{mol/Lh}{mol/Lh}\right]$	$Y_{\frac{acetate}{H_2}}$ $\left[\frac{mol/Lh}{mol/Lh}\right]$	$Y_{\frac{H_2}{CO_2}}$ $\left[\frac{mol/Lh}{mol/Lh}\right]$	HTR $[mol/Lh]$	$\frac{HTR}{HUR}$ $\left[\frac{mol/Lh}{mol/Lh}\right]$
A	0.039	0.019	0.423	0.182	2.053	0.033	0.846
B	0.035	0.025	0.304	0.208	1.400	0.034	0.971
C	0.014	0.005	0.775	0.277	2.800	0.025	1.786
D	0.012	0.006	0.703	0.386	2.000	0.013	1.083
E	0.012	0.007	0.664	0.359	1.714	0.013	1.083
F	0.02	0.024	0.177	0.210	0.833	0.014	0.700

4.2.1. Discussion

A proper calibration and/or check of the offgas analysers as well as the mass flow controllers prior to every fermentation is of great importance. Furthermore the deviations for stripped acetate and steam were evaluated to correct the carbon and DoR balances properly.

The pH equilibrium for acetate, the intermediate acetate concentration and the cultivation temperature led to the conclusion, that the acetate losses due to evaporation, can be neglected. However, the high offgas temperature causes approximately 3,3 % water concentration in the offgas. This has to be included in the overall gas balance. As table 4.4 shows, the balances for carbon and the degree of reduction still does not sum up perfectly but are appropriate.

All cultivations showed a lag-phase between 12 to 15 h for both growth and acetate production. The maximum achievable biomass concentrations varied between 0.8 and 1.2 g/L. The highest reached acetate titers were measured for experiments B and C with 24.2 g/L. Throughout all cultivations only acetate and small amounts of formate were detectable. It seems that bad mass transfer, hence small gas uptake rates promoted the formation of formate and as soon as the substrate availability is high enough formate is further metabolised.

The uptake rates after the gas switching in continuous cultivation (experiment F; see figure 4.8) shows a distinct deviation from the expected HUR/CDUR ratio or $Y_{\frac{H_2}{CO_2}}$ of two, based on the stoichiometry (equation (2.2) of the Wood-Ljungdahl pathway [51]). It seems that this does not affect neither growth nor acetate formation (see figure 4.7) in any way. This could be a sign of a carbon dioxide saturation effect as a result of the higher driving force. However, a possible following normalization was not identifiable due to the depleted feed media. Further testing of gas switching effects and influences must be considered.

The uptake rate curves show some noise for the experiments B to F. This may be a

result of the small differences of hydrogen and carbon dioxide between in- and offgas concentrations. This also reveals potential optimization for gassing rate control. A feasible control approach could be the variation of the gassing rate in relation to a small residual CO_2 offgas concentration of 0.5 %. This would also contribute to the desired, almost carbon free offgas.
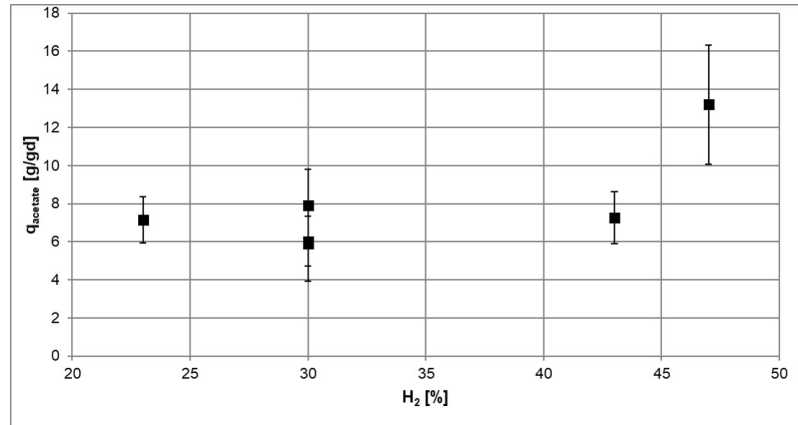

Figure 4.9.: Trend for all biomass specific reaction rates $q_{acetate}$ over hydrogen concentration

The figure 4.9 shows a clear trend for the biomass specific reaction rate $q_{acetate}$. The highest hydrogen concentration resulted in a significantly higher $q_{acetate}$ of 13.2 g/g d, but in the same range as the literature values presented in table 4.2. In contrast to that, any variation for all lower hydrogen concentrations provoke no significant change in the reaction rate. This could indicate a mass transfer limitation for hydrogen. This presumption is also supported by the HTR/HUR ratios (ranging between 0.7 and 1.8) displayed in table 4.5. In comparison, the possible carbon dioxide transfer rate is on average 240 times higher than the carbon dioxide uptake rate.

In addition, Demler et.al. [15] showed a complete depletion of the amino acids L-tryptophan and L-asparagin from the complex media (yeast extract). Unfortunately not all amino acids were evaluated in these tests. A screening for all amino acids throughout *A. woodi* cultivations should be considered to determine further media limitations.

Due to possible inhibitions or bottlenecks of the involved enzymes for the terminal steps in the acetyl-CoA-pathways, genetically engineered *A. woodii* strains could improve performance. The over-expression of the four tetrahydrofolate (THF) dependant enzymes (see figure 2.2) of the methyl branch as well as the over-expression of the phosphotransacetylase and the acetate kinase to enhance formate processing and ATP- generation provided no meaningful improvements in the biomass specific reaction rate $q_{acetate}$ but increased μ on average by 66 % [15], [36], [60].

A final fermentation in F11 was planned and started, to demonstrate and evaluate the physiological influences and productivity for gas switching procedures especially because these are highly possible within an industrial setting as well as the higher hydrogen concentrations/partial pressure. In addition, the effects of carbonate, already tested in small scale serum bottles (see section 4.3.1), should be determined in a pH controlled setting.

Unfortunately this failed and was the initial hint for the possible contamination explained in section 4.4 in more detail. Furthermore specific inhibitory effects, which are of great interest, could not be assessed due to these contamination issues.

4.3. Serum bottle experiments

Small scale experiments were carried out in rubber sealed 125 mL serum bottles. The applicability of a minimal media and physiological needs regarding media composition were tested.

In addition, the inhibitory effects of gas components such as oxygen and carbon monoxide, and the respond of *A. woodii* to this were determined.

This useful method can give first hints which can later be tested and monitored in a completely controlled fermenter setting.

4.3.1. Minimal media and substrate testing

A defined media without any complex substrate components (e.g. yeast extract, protein hydrolyzate (peptone, casein), etc.) is preferred due to an easier analysis and determination for physiological requirements. An extensive research led to an already researched and applied defined media for *A. woodii*. It was published by Heise et.al. [28] and can be seen in table 3.2. Nevertheless, Demler et.al.[15] showed the necessity of yeast extract in the media despite the addition of possible limiting amino acids (L-Asparagin and L-Tryptophan).

The product formation and the growth rates were therefore compared for this minimal media and the standard complex media. Additionally the effects of carbonate as a buffer and different sugar as a carbon source were tested.

Both media were examined in a sodium carbonate containing and carbonate free version. For the media without carbonate, the necessary Na^+ concentration of 50 mM was provided with NaCl instead.

Mixotrophic experiments were executed with the suggested sugar fructose as well as with glucose in a final concentration of 10 g/L.

The utilized headspace gas atmosphere was a mixture of 80 % hydrogen and 20 % carbon dioxide at 1.0 bar overpressure. The duration of cultivation was 48 h, at this point the biomass concentration had reached a steady state.

Unfortunately there was no growth or metabolite production observable for the defined minimal media. Even a reiteration with a new preculture produced similar results.

The results for the tested metabolites (figure 4.10) in mixotrophic conditions show a clear difference between carbonate and non carbonate containing media.
The consumption of fructose in the carbonate free media is not significantly different from zero but was 3.4 g/L for the carbonate containing media. Furthermore the titers of both formate and acetate are significantly lower as well for the carbonate free media with 0.19 g/L for formate and 0.10 g/L for acetate. The carbonate containing media in comparison shows concentrations of 0.51 g/L for formate and 0.15 g/L for acetate. The growth rate for the carbonate free media is 0.0033 h^{-1} and therefore less than half as it is for the carbonate containing media with 0.0087 h^{-1}. Unexpectedly high lactate concentrations of 3.87 g/L for the carbonate containing media, 1.15 g/L for the carbonate free media and 6.08 g/L for glucose were measured.

In contrast to that, the autotrophic tests show quite similar results independent from the carbonate. The concentrations for the carbonate containing media is slightly higher but the yields are similar. The final metabolite titers for lactate range between 0.31 and 0.32 g/L, for formate between 0.07 and 0.09 g/L and for acetate between 0.14 and 0.17 g/L.
This could simply be the result of the higher availability of dissolved carbon dioxide due to the carbonate, meaning a slightly higher overall carbon activity. In addition, the growth rates vary in the area of 0.00146 to 0.00155 h^{-1} but not significantly.

The biomass specific acetate reaction rates do not vary significantly for either mixotrophic or autotrophic conditions. The autotrophic conditions resulted in a higher average $q_{acetate}$ of 0.087 g/g d in comparison to the mixotrophic conditions with 0.022 g/g d. One has to take into account that the standard errors are in the same range as the reaction rates for mixotrophic conditions, therefore smaller standard errors could alter these results. The autotrophic acetate reaction rates are more than four times

higher than the mixotrophic ones.

The different carbon sources for mixotrophic conditions had an impact as well. The product concentration for formate with 0.33 g/L is clearly lower and the biomass specific acetate reaction rate $q_{acetate}$ with 0.0098 g/g d is lower for glucose. The acetate titer of 0.16 g/L is however in the same area. In contrast to that, the growth rate of 0.0134 h^{-1} is 34% higher with glucose as the carbon source. Additionally, the final biomass concentration of 0.65 g/L for glucose was higher than for fructose with 0.42 g/L.

There are unexpected high titers of lactate in all samples, as the figures 4.10 and 4.11 show. For mixotrophic conditions this could be a sign of an incomplete glycolysis. The presence of lactate in autotrophic conditions is more worrying.
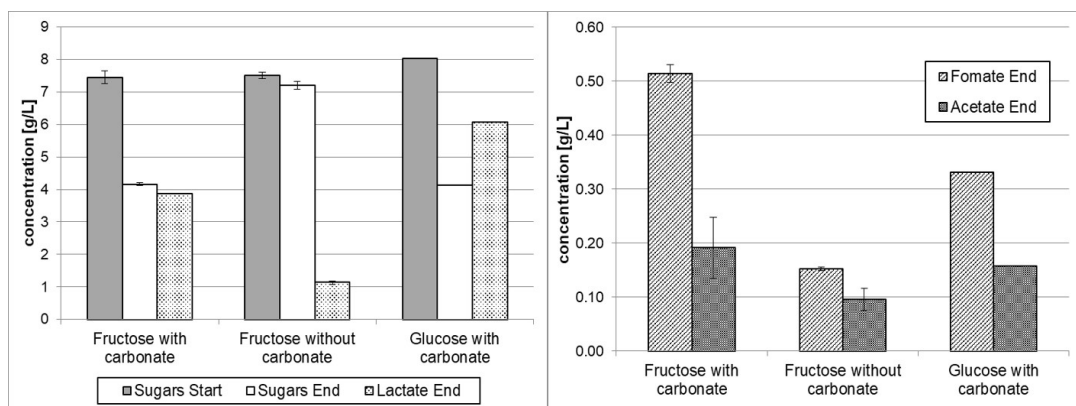
Figure 4.10.: Measured product concentrations for mixotrophic growing conditions for complex media
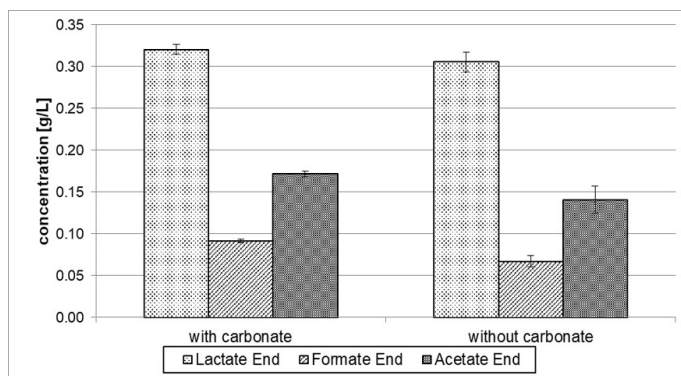

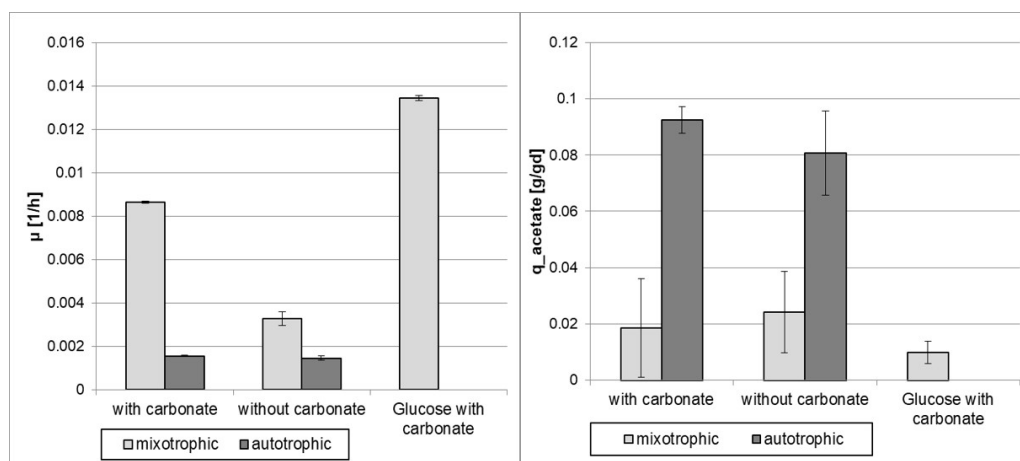Figure 4.11.: Measured product concentrations for autotrophic growing conditions for complex media

Figure 4.12.: Growth rates μ and specific reaction rates $q_{acetate/X}$ for the media test

Discussion

These results are contradictory to the publication Heise et.al. [27] on the sodium dependence of *A. woodii* controlled with NaCl as the sole Na$^+$ source. The highest researched concentrations in that paper were 20.9mM NaCl. This leads to the suspicion, that the higher overall salinity of 50mM NaCl negatively affected the fructose consumption, the acetate production and the growth rate.

The differences for the biomass specific acetate reaction rate between mixotrophic and autotrophic conditions is presumably caused by the higher final biomass concentration and the high titers of lactate in the mixotrophic serum bottles.

The sugar test results led to the decision to exchange fructose with glucose as the carbon source for further precultures and mixotrophic experiments due to the higher obtained biomass concentration.

Demler [15] tested the effects of acetate concentrations for potential inhibitory effects and additional metabolite formation. The results showed first signs of negative influence on growth and product formation at 5 g/L acetate and a severe inhibition for acetate concentrations above 30 g/L. It is suspected that this is a result of the inhibition of the enzym acetate kinase and therefore a blockage of the Acetyl-CoA-pathway [15].

It is presumed, that *A. woodii* has an alternative metabolism to produce energy in the presence of high acetate concentrations or low pH values. This competence was not reported yet, but the genome analysis showed the presence of such a lacatate-dehydrogenase [55].

Nevertheless, under the tested conditions it is unlikely that *A. woodii* produced lactate in these high concentrations. This lead to the suspicion of a contamination of unknown origin throughout this test.

4.3.2. Oxygen inhibition test

Karnholz et.al. [37] tested five different facultative anaerobic acetogens on their physiological and metabolic response to gaseous oxygen. The observed results were, that *A. woodii* and *Thermoanaerobacter kivui* were the most sensitive ones towards oxygen and they did not grow in a nonreduced medium. *A. woodii* was inhibited completely when oxygen in the gas phase exceeded 0.3 vol% [37].

For these reasons the inhibitory effects of the oxygen concentration in the headspace as well as the upper limit for complete inhibition were examined. Furthermore the respond of *A. woodii* in mixotrophic and autotrophic media under non anaerobic conditions was evaluated.

Mixotrophic conditions were executed with glucose in a final concentration of 10 g/L.

The utilized headspace gas atmosphere was the varying criterion for this experiment. Six different gas mixtures at 1.0 bar overpressure were applied (for detailed composition of OMV gas mixture see table 3.3):

1. OMV gas mixed with 30% H_2 to a final O_2 concentration of 1.8 % (8.6 % CO_2)

2. OMV mixed with N_2 and 30 % H_2 to a final O_2 concentration of 0.6 % (2.8 % CO_2)

3. OMV mixed with N_2 and 30 % H_2 to a final O_2 concentration of 0.3 % (1.4 % CO_2)

4. OMV gas mixture (2.56 % O_2, 11.9 % CO_2, 0 % H_2)

5. 100 % N_2

6. Recommended standard gas mixture with 80 % H_2 and 20 % CO_2 as control

The cultivation and sampling was carried out until each biomass concentration reached a steady state.

Mixotrophic conditions

The mixotrophic growth shows a fairly uniform trend for the different gas mixtures (figure 4.13) with a steady state biomass concentration of approximately 1 g/L. The glucose consumption and the product formation does not vary strongly between the six different gas mixtures. The glucose consumption for gas with the highest O_2 contents (gas 5) is clearly higher with 4.91 g/L and for the control (no oxygen, gas 6) noticeably lower with 1.85 g/L whilst all other gases have an average glucose consumption of 2.9 g/L.

High concentrations of lactate, on average 4.0 g/L, were obtained independent of the gas mixtures except the nitrogen only serum bottle where it was 3.0 g/L.

The final acetate concentration of 0.69 g/L for gas 4 (highest O_2 content of 2.56 %) is significantly higher than all others which vary between 0.45 and 0.52 g/L.

The reaction rates are quite uniform (on average 0.16 g/g d) for all gases, only for gas mixture 4 (highest O_2 content) it is 20 % higher with 0.20 g/g d.

The growth rates vary noticeably more, ranging from 0.037 to 0.067 h^{-1}. Unexpectedly, there is no particular trend, in respect to the oxygen concentration, identifiable.

Autotrophic conditions

The autotrophic growth shows a distinct spread in the trends for the different gas mixtures (figure 4.15). There is a constant decrease in the biomass concentration for autotrophic conditions identifiable. A microscopic check revealed this as a flocculation which was probably caused by a low pH or the steady state in the serum bottle. Also the highest reached biomass concentrations varied between 0.12 and 0.2 g/L.

The highest observed acetate concentration is 0.45 g/L for the gas mixture with the highest oxygen and carbon dioxide concentration (gas 1). The other oxygen containing gases are lower but do not differ significantly from another. It stands out, that there are unexpected metabolites, 0.15 g/L acetate and 0.14 g/L formate for gas 5 (only N_2), although there are not any substrates present. This could be a result

of the provided complex media component (yeast extract) and/or trace amounts of organic compounds from the pre-culture.

The formation of lactate in concentrations of up to 1.0 g/L in the control serum bottle and 0.64 g/L on average in the oxygen containing serum bottles is unexpected for *A. woodii* in these conditions.

The reaction rates vary between 0.5- 0.65 g/g d for all gases except gas 5 (only N_2), were it is approximately 50% lower with 0.26 g/g d. This seems plausible because there is not any proper substrate, as already mentioned above, available.
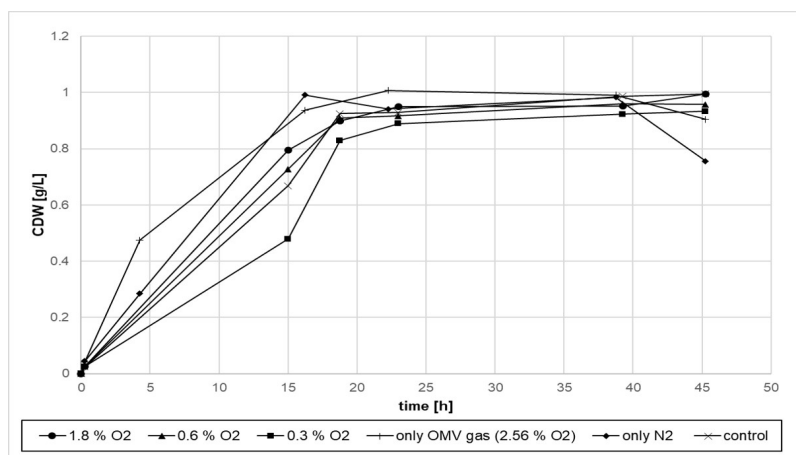
Figure 4.13.: Growth trends for mixotrophic growing conditions with oxygen containing gases
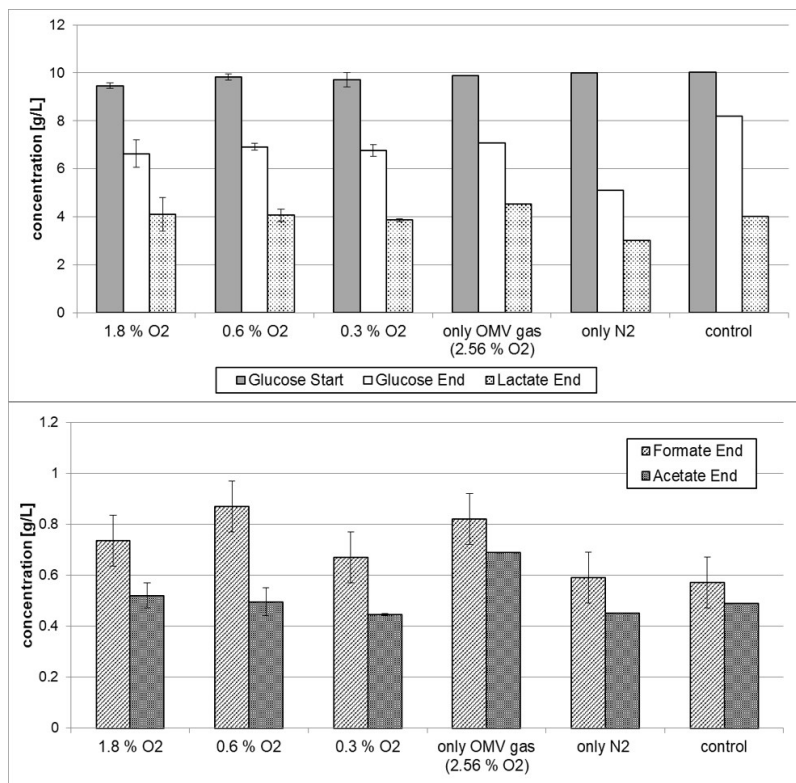

Figure 4.14.: Measured product concentrations for mixotrophic growing conditions with oxygen containing gases
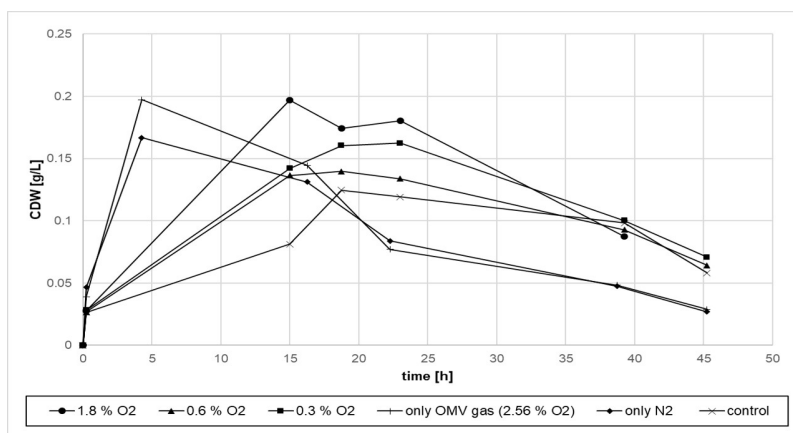
Figure 4.15.: Growth trends for autotrophic growing conditions with oxygen containing gases
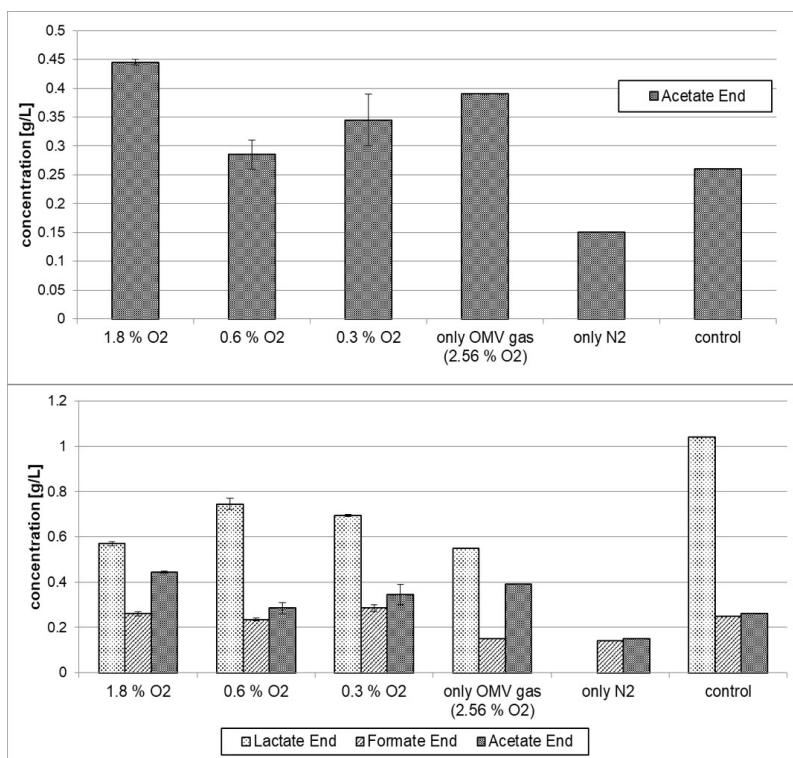
Figure 4.16.: Measured product concentrations for autotrophic growing conditions with oxygen containing gases
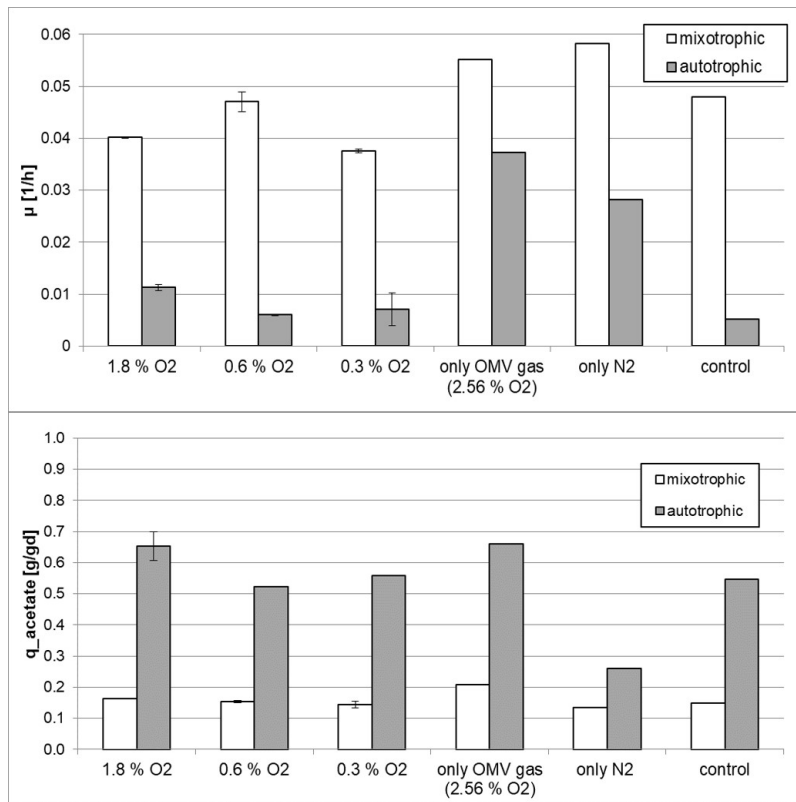
64

Figure 4.17.: Growth rates μ and specific reaction rates $q_{acetate/X}$ for the for oxygen containing gases

Discussion

It is important to mention that the final gaseous CO_2 concentrations in the headspace are low ($<3\%$) for the intensely diluted OMV gas mixture.

The steep initial autotrophic curves for gas mixtures 5 and 6 originate from the fact that these serum bottles were inoculated later from a potentially already growing fresh preculture. This has to be considered in the interpretation of the rates (figure 4.17).

In consideration of that, the growth rate is the highest for gas 4 with the highest oxygen content. The growth rates also decrease for lower oxygen concentrations, even though this trend is not significant. This is completely conflicting with the oxygen limit mentioned in Karnholz et.al.[37].

In addition the high titers of lactate in all samples (see figures 4.14 and 4.16) are alarming.

As already mentioned in section 4.3.1 there are possible physiological ways for *A. woodii* to produce lactate but under the tested conditions it is unlikely that lactate is produced in these high concentrations. Even for mixotrophic conditions and the consideration of an incomplete glycolysis this does not seem plausible. This lead to the suspicion of a contamination of unknown origin throughout this test and the identification of the potential contamination described in section 4.4.

4.3.3. Carbon monoxide inhibition test

For the fixation of carbon monoxide, the Wood-Ljungdahl pathway is utilized in acetogens as well. CO is also one of the major components in the OMV gas mixture (see table 3.3) just as in synthesis gas [20]. Several anaerobic acetogens are known to grow on CO or syngas.

Bertsch and Müller [7] reported, that *A. woodii* does not grow on fructose-CO or CO alone but a combined metabolism of CO is possible if H_2 and CO_2 are available. When more than 25 % CO was present in the gas phase, fructose utilization was completely inhibited and the acetate productivity dropped to 10 % immediately. Furthermore, the autotrophic usage of H_2 did not start until almost all of CO was consumed. The productivity was also reduced by 20 % and the growth rate was 4.5 times lower for CO concentrations between 5 and 15 % [7].

At high cell densities, the consumption of CO can be high enough that the concentration of solubilized CO is low enough to allow simultaneous H_2 oxidation. However, an optimization of such a process might lead to inhibition of CO-sensitive hydrogenase and therefore lower H_2 consumption [6]. Furthermore the CO_2 reduction, catalysed by the HDCR, is a bottleneck for acetate formation with CO as the electron donor [7]. A simultaneous consumption of H_2 and CO reported in several publications could be explained with the poor solubility of CO as described in section 2.4.1.

On these grounds the inhibitory effects of higher carbon monoxide concentrations in the headspace and the following respond of *A. woodii* were tested.

Mixotrophic conditions were executed with glucose in a final concentration of 10 g/L.

The utilized headspace gas atmosphere was the varying criterion for this experiment. Eight different gas mixtures at 1.0 bar overpressure were applied (for detailed composition of VOEST gas mixture see table 3.3):

1. VOEST gas mixture (25.4 % CO, 22.9 % CO_2, 4.0 % H_2)

2. VOEST mixed with 30 % H_2 to a final CO concentration of 18,8 % (16.9 %

CO_2)

3. VOEST mixed with N_2 and 30% H_2 to a final CO concentration of 15 % (13.5 % CO_2)

4. VOEST mixed with N_2 and 30% H_2 to a final CO concentration of 10 % (9.0 % CO_2)

5. VOEST mixed with N_2 and 30% H_2 to a final CO concentration of 5 % (4.5 % CO_2)

6. VOEST without CO (22.9 % CO_2, 4.0 % H_2)

7. VOEST without CO and mixed with 30 % H_2 (16.9 % CO_2)

8. Recommended standard gas mixture with 80 % H_2 and 20 % CO_2 as control

The cultivation and sampling was carried out until each biomass concentration reached a steady state.

Mixotrophic conditions

The steady state biomass concentration varied between 0.85 and 1.1 g/L. The sugar consumptions is on average 5.4 g/L and the lactate formation averages 5.5 g/L and both are fairly uniform throughout all gas mixtures (see figure 4.19). These are the highest observed lactate concentrations throughout all serum bottle tests.

There is a pronounced trend for the final metabolites formate and acetate visible. There is no formate detectable for the three highest CO concentrations (gases 1-3). For the gases with 10 and 5 % CO (gases 4 and 5) 0.05 g/L and for the CO free gas mixtures and the control (gases 6,7 and 8) 0.25 g/L formate are present.
Also the acetate concentration only starts to increase significantly for CO amounts of 5 % and below. The control and gas 5 (5 % CO) show the same slightly lower acetate titers of 0.16 g/L in comparison to the CO free gas mixtures (gases 6 and 7) with 0.22 g/L.

68

The growth rates and the reaction rates show a similar result but the growth rates for gases with a low CO ratio (gases 5,6 and 7) do not vary significantly with 0.051 h^{-1} on average.

The biomass specific reaction rates for the CO free VOEST gases 6 and 7 are significantly higher with 0.70 g/g d in comparison to all others. The control and all CO containing samples range between 0.12 and 0.22 g/g d.

Autotrophic conditions

The autotrophic growth shows a very distinct spread in the trends for the different gas mixtures. The CO containing serum bottles produced approximately 0.16 g/L biomass concentration while the CO free gases yielded slightly higher with 0.21 g/L. There is also a constant decrease in the biomass concentration identifiable. A microscopic check revealed this as a flocculation which was probably caused by a low pH or the steady state in the serum bottle. This starts later with higher CO concentrations, due to the possibly slower metabolism.

The acetate formation shows no specific relation in respect to the CO content with an average concentration of 0.17 g/L. There was no formate detectable for all CO containing gas mixtures but 0.1 g/L for the CO free serum bottles.

The lactate concentrations are significantly higher for the autotrophic CO containing samples with approximately 0.42 g/L in comparsion to the CO free bottles with 0.18 g/L. The control also yielded an unexpected high lactate titer of 0.36 g/L.

The growth rates are approximately two times higher with 0.011 h^{-1} for the samples without CO in the atmosphere. It stands out, that the control serum bottle is in the same area with 0.006 h^{-1} as the CO containing samples.

Moreover the reaction rates show no certain trend, but start to increase with 1.50 g/g d for gas 5 (5 % CO) and are significantly higher with an average of 2.15 g/g d (1.5 to 2 times) for the samples without CO.
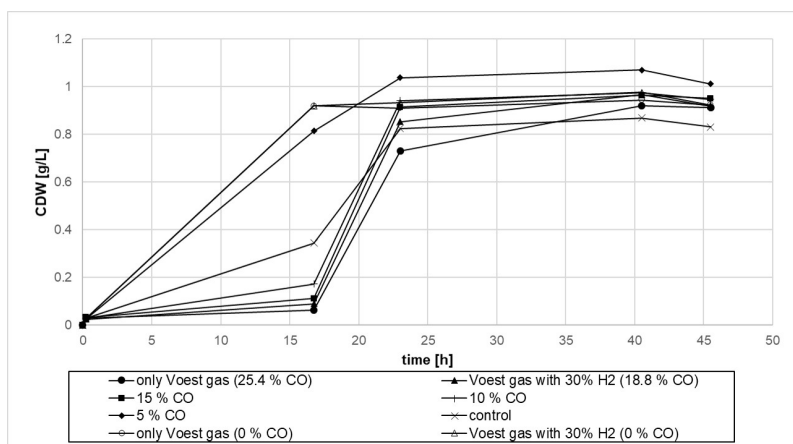
Figure 4.18.: Growth trends for mixotrophic growing conditions with carbon monoxide containing gases
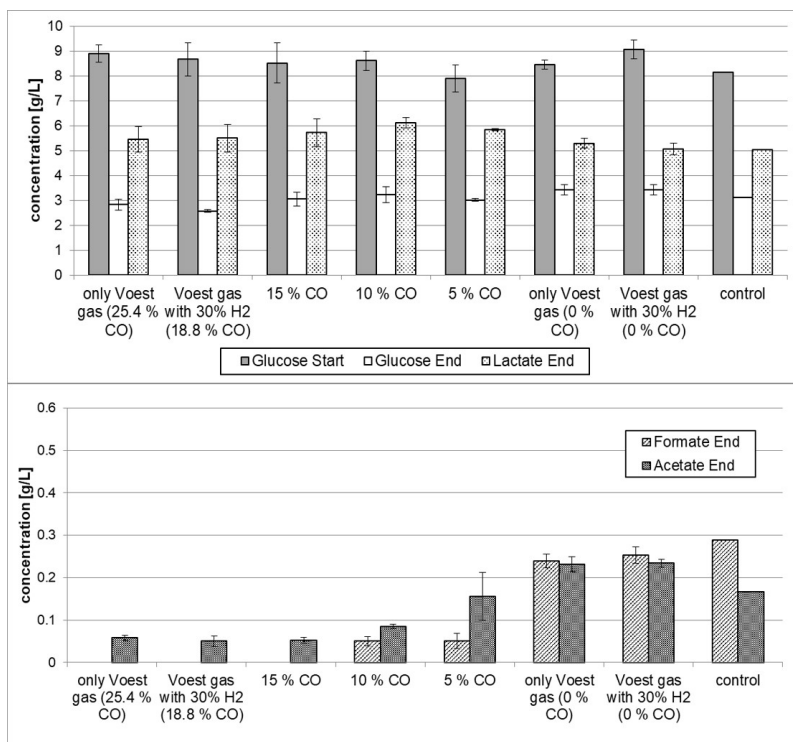

Figure 4.19.: Measured product concentrations for mixotrophic growing conditions with carbon monoxide containing gases
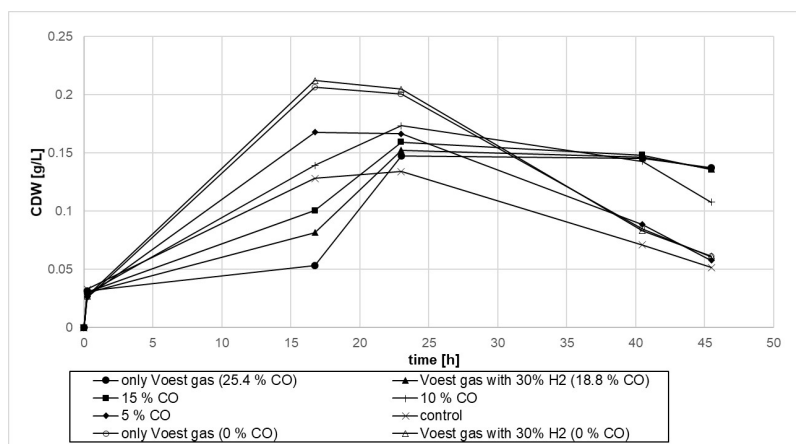
70

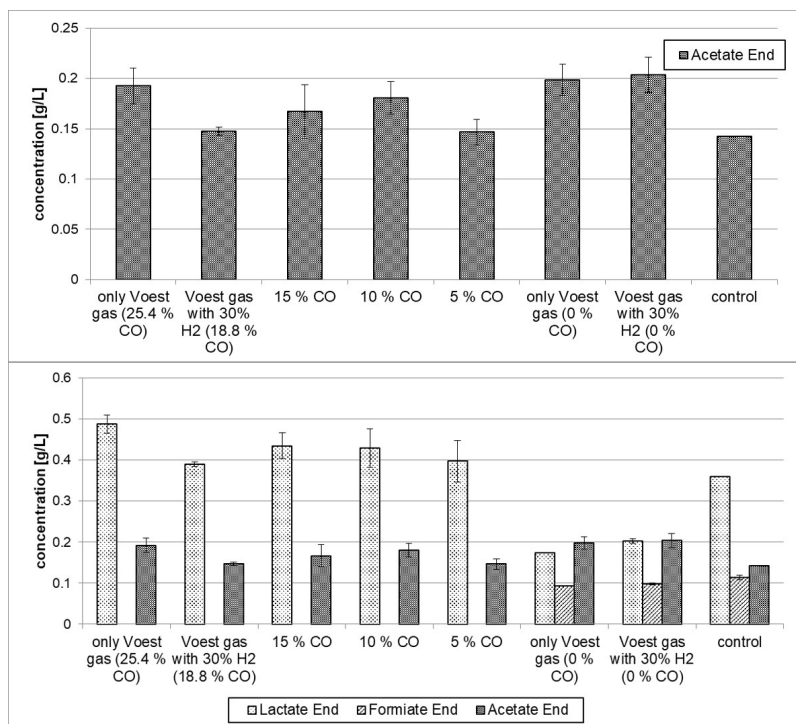Figure 4.20.: Growth trends for autotrophic growing conditions with carbon monoxide containing gases

Figure 4.21.: Measured product concentrations for autotrophic growing conditions with carbon monoxide containing gases
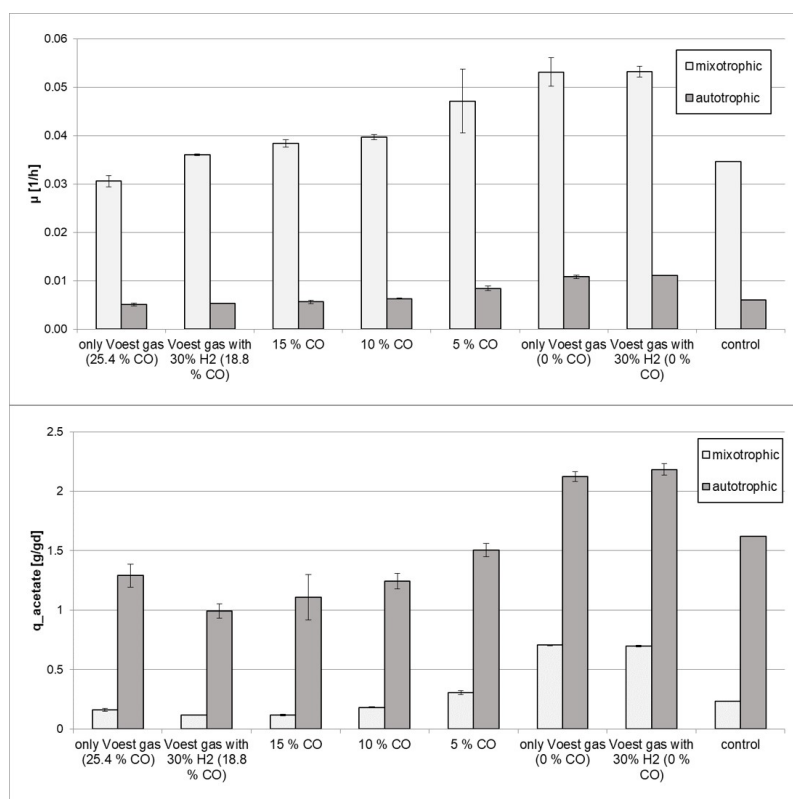
Figure 4.22.: Growth rates μ and specific reaction rates $q_{acetate/X}$ carbon monoxide containing gases

Discussion

The growing phases for all CO containing gases (gases 1-5) had distinct longer lag-phases for both mixotrophic and autotrophic conditions.

Interestingly, the control (gas 8) is in the same range as the sample with the highest CO concentration for both growth rate and biomass specific reaction rate as well as for both mixtrophic and autotrophic conditions.

Additionally, there are high titers of lactate in all samples (see figures 4.19 and 4.21). Previous publications [7] [14] showed no noticeable lactate formation for *A. woodii* cultivations with CO.

As already mentioned before, it is possible for *A. woodii* to produce lactate through a possible lacatate-dehydrogenase pathway [55] but under the tested conditions it is unlikely that lactate is produced in these high concentrations. Though a strong CO

inhibition of the last steps of the Acetyl-CoA-pathway is known for *A. woodii* [7]. However, the previously mentioned possible contamination seems to be more plausible. The identification of the potential contamination is described in section 4.4.

4.3.4. Conclusion

The growth rates for all serum bottle experiments were not unexpectedly high (ranging between 0.005 and 0.05 h^{-1}) and were in the same region as the growth rates for the cultivations 4.2. Therefore a possible contamination was not obvious.

Nevertheless, high lactate concentrations throughout all serum bottle tests strongly indicate a potential contamination.

All serum bottle cultures were discarded before the potential contamination was noticed and therefore could not be tested for the other mircoorganisms. The same cryo stocks as described in section 4.4 were used for these tests. The obtained results do not fit the expected behaviour of an *A. woodii* cultivation with the presence of the inhibitory components oxygen or carbon monoxide. The validity of the results is therefore doubtful. A reiteration of these experiments is highly recommended.

4.4. Identification of the potential contamination

As already mentioned in section 4.2 and 4.3 a contamination potentially occurred.

A suspiciously long lag-phase of 20 hours occured despite proper *A. woodii* autotrophic cultivation conditions in a started and planned fermenter F11 cultivation. A glucose peak was added to accelerate or end the lag-phase and it led to an immediate growth and base consumption. Additionally, there was neither a hydrogen nor carbon dioxide uptake but a slight carbon dioxide emission observable. There was no autotrophic growth possible and therefore the surmise of a contamination with a strict or facultative anaerobic but not autotrophic microorganism.

A HPLC evaluation indicated acid fermentation metabolites (lacate, acetate, ethanol, formate and succinate). The product yields bring *E. coli* in the focus for anaerobic conditions [24] but other microorganisms are possible.

The investigation for the probable cause was made by a combined serum bottles dilution series, a colony-PCR and a Gram-staining. Figure 4.23 shows the scheme for the dilution series. All serum bottles were carried out in 125 mL bottles filled with complex media 3.1 and a headspace atmosphere with 80 % H_2 and 20 % CO_2 at 1.3 bar overpressure. For mixotrophic conditions glucose was added to a final concentration of 10 g/L. Sodium sulfite was added accordingly the original media A.1 to maintain a lower redox potential and therefore enhance the selection pressure. The bottles A to D were inoculated from the same cryo-stock. As soon as there was either gas consumption (lower headspace pressure) or significant acetate concentration noticeable a new serum bottle was further inoculated with that specific culture.

The serum bottles E and F showed high titers of acetate (4.3 g/L) and were therefore used for the colony-PCR and Gram- staining. Approximately 4 g/L of acetate were also produced in the pre-cultures of the properly accomplished fermentations (see section 4.2). Additionally, a fractionated streaking of those cultures in petri dishes (DSMZ135 A.1 with 15 g/L agar) was carried out.
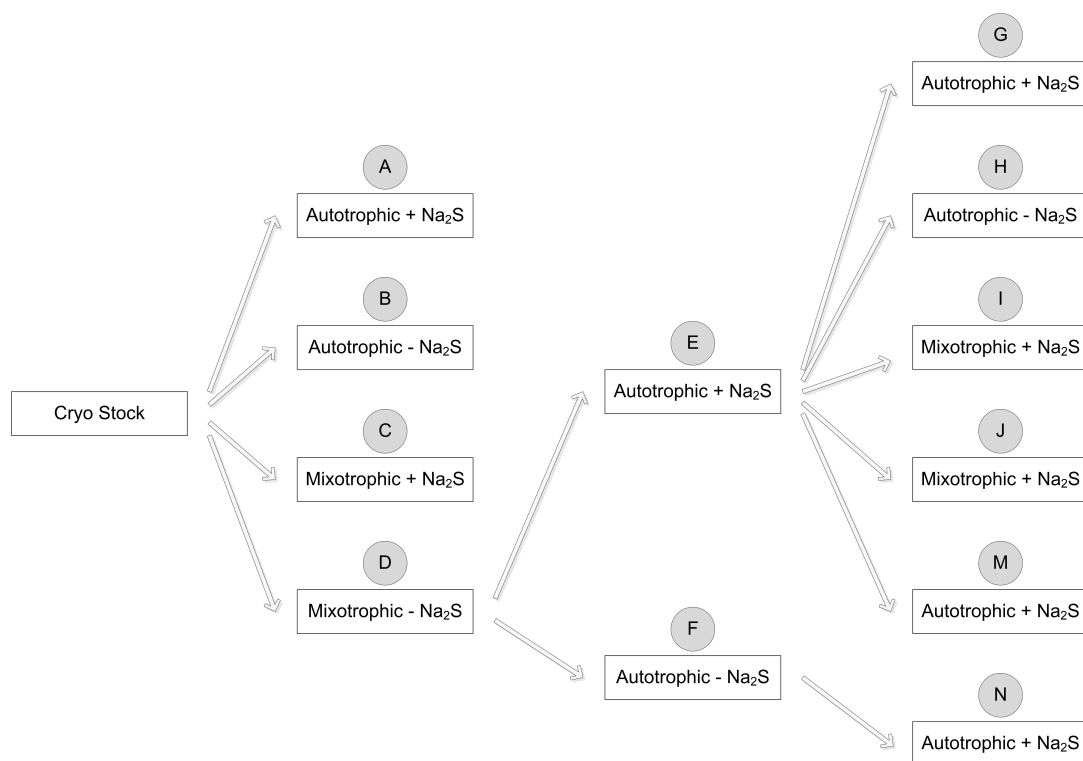
Figure 4.23.: Serum bottle dilution series scheme for contamination screening

Three different Colony-PCRs resulted in completely contradictory results and were therefore not respected.

The Gram-staining was performed with *Lactobacillus plantarum* as a positive and *Escherichia coli* as a negative control. Furthermore the serum bottles and the resulting petri dishes for E and F as well as an initial cryo stock were tested.

Table 4.6.: Results from Gram-staining

Strain	Gram staining
L. plantarum	uniform, Gram positive
E. coli	uniform, Gram negative
Serum bottle E	contamination, 30 % Gram positive
Serum bottle F	contamination, 50 % Gram positive
Petri dish E	uniform colony 50:50 Gram positive/negative
Petri dish F	uniform colony, 50:50 Gram positive/negative
Cryostock	contamination, 20 % Gram negative (possibly *E. coli*)

Discussion

The suspicion of a contamination seems to be confirmed. The likely starting point and mutuality is the cryo-stock.

The continuous process of several serum bottle cultivation and reinoculation (see figure 4.23) as described above should help to achieve a pure culture of *A. woodii* again.

It is assumed that all serum bottle experiments were affected by that same contamination. The obtained results are considered highly questionable.

The fermentations are likely not to be affected due to an older cryo stock for precultures. Additionally, the obtained results match published results and expectations considerably better.

4.5. On-line data processing and acetate soft sensor

Lucullus PIMS provides a wide range of possible process improvements and easier data processing. A practical utilization of on-line data processing and soft sensors was assessed for *A. woodii* cultivations as well as the the whole Power-To-Product process.

The goal for on-line data processing was, to have most results (such as specific and volumetric rates, base rate, yields, etc.) accessible during the running cultivation to notice trends early on and make experiments more convenient and therefore more industry ready.

The main challenges for this are on-line biomass and metabolite measurements as well as gaseous mass transfer. A suitable concept for mass transfer is already presented in section 4.1.

4.5.1. On-line biomass

An online turbidity probe 316L (Fogale nanotech, Nimes, France) with a wavelength of 880 nm was applied and tested for applicability.

Due to limited *A. woodii* availability, a finished *E. coli* fermentation was utilized for this test. Furthermore the cell density range could be chosen broader as well.

A three-dimensional Design of Experiment concept (see table 4.8) was applied with a following multi-linear statistic evaluation.

Table 4.7.: Design of Experiment normalized set-points

	Agitator speed [min^{-1}]	Gassing rate [L/min]	Biomass concentration [g/L]
-1	400	0.338	0.6
0	700	0.563	3.3
1	1000	0.788	6.0

Table 4.8.: Design of Experiment table for multi-linear regression model for the biomass function with different cultivation settings

Experiment	Agitator speed	Gassing rate	Biomass concentration
1	-1	-1	+1
2	+1	-1	+1
3	0	0	+1
4	-1	+1	+1
5	+1	+1	+1
6	0	+1	0
7	0	0	0
8	+1	0	0
9	0	0	0
10	-1	0	0
11	0	0	0
12	0	-1	0
13	-1	-1	-1
14	+1	-1	-1
15	-1	+1	-1
16	+1	+1	-1
17	0	0	-1
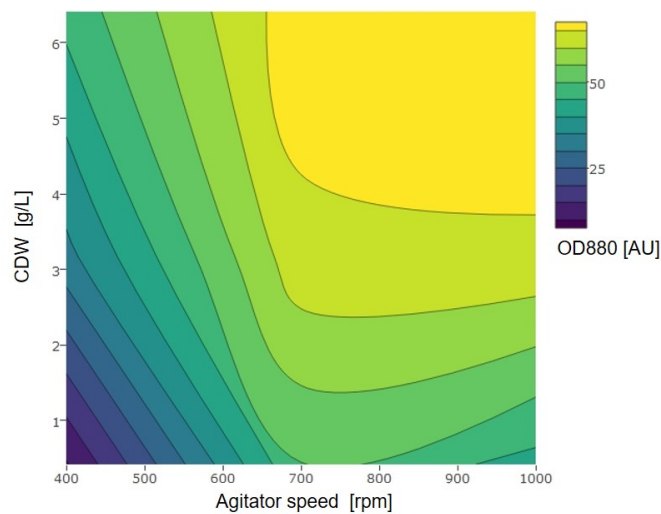
Figure 4.24.: Contour plot of the measured data points

78

Before analysis, there was a distinct smoothing of the obtained raw OD_{880} measurements necessary. The statistical data analysis and the multi-linear regression for a fitted model was carried out in Rstudio.

This resulted in the removal of the gassing rate from the model due to a non-significant statement on a 10 % significance level. In addition, this adjustment improved the goodness of fit R^2 by 9.5% for the final model (equation (4.6)).

$$CDW\,[g/L] = 0.119 \cdot OD_{880}\,[AU] - 0.056 \cdot Agitator\,speed\,[min^{-1}] \tag{4.6}$$
$$model\,fit\,R^2 = 58.2\,\%$$

Discussion

As the final goodness of fit, R^2, in equation (4.6) shows, the linear model is far-off from a proper estimation of the real circumstances. The contour plot of the measured DoE data points (figure 4.24) shows severe non-linearities for higher agitator speeds. It seems that there is no influence on the OD_{880} for agitator speeds above 750 rpm at all.

This led to the conclusion that this biomass sensing method is not practical for our application. A conductivity measurement for the biomass determination could provide a better solution, but due to missing applicability and availability this was condemned.

4.5.2. Acetate soft sensor

During data evaluation a distinct relation between acetate formation and consumed base for pH control stood out. In this case, a data driven black-box-model [13] was applied for the acetate soft sensor measurement. A linear regression of the collected produced acetate and consumed base data provides an easy soft sensor approach for an on-line acetate concentration monitoring during cultivations.

$$m_{acetate}\,[g] = 0.2399 \cdot m_{base}\,[g] \tag{4.7}$$
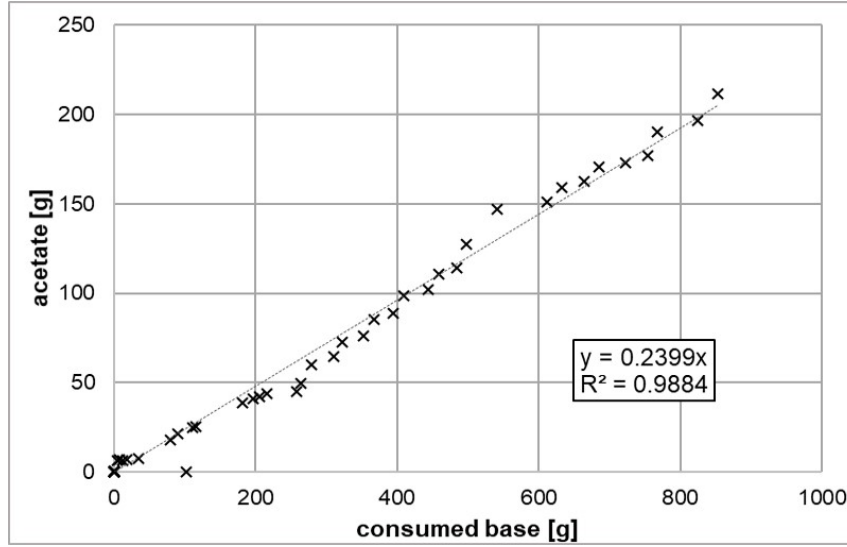
$$model\ fit\ R^2 = 98.8\,\%$$

Figure 4.25.: Linear regression for produced acetate over consumed base

The amount of produced acetate $m_{acetate}$ in accordance to the model (4.7) above was incorporated as a calculator in Lucullus PIMS with regards to the manufacturers manual [9]. The calculator performed with 99.1 % accuracy in relation to offline HPLC data (continuous cultivation experiment).

Subsequently, the yields $Y_{\frac{H_2}{CO_2}}$, $Y_{\frac{acetate}{CO_2}}$ and $Y_{\frac{acetate}{H_2}}$, the gas uptake rates HUR and CDUR (equation (2.25)), the gas transfer rates HTR and CDTR (due to the models (4.3) and (4.4)) and the base rate were also incorporated as online calculators in Lucullus PIMS.

Unfortunately, due a contamination of the preculture and the ensuing failed F11 fermentation, there was no possibility to test the online calculators and their efficient functioning.

5. Summary

Throughout almost all industrial processes, carbon dioxide is produced and subsequently emitted into the atmosphere. This results in an anthropogenic ecological footprint which cannot be sustained by the earth forever. The handling of those waste gas flows is highly important and could provide great future value.

Acetobacterium woodii, as a carbon dioxide reducing organism, is suitable for this task even though process intensification is not at a maximum yet. The complex composition of industrial flue gases with inhibitory components must be further addressed in order to enable an industrial applicability. If a direct flue gas utilization is not applicable, an upstream gas cleaning or separation could help to provide suitable gas conditions.

Due to all progress, it seems plausible, that the wild strain of *Acetobacterium woodii* has a maximum biomass specific acetate reaction rate $q_{acetate}$ somewhere near 18 to 22 g/g d and therefore an improvement of the overall productivity is only possible when targeting the increase of volumetric reaction rates.

The observable limitations concerning mass transfer could be addressed with an increase in the hydrogen concentration at ambient pressure conditions. The coupling with a gas permeation based gas recycling system appears to be the most sustainable and advantageous solution [46]. This approach could also support the demand for carbon free industrial flue gases.

In addition, an over-expression of the hydrogen-dependant CO_2 reductase HDCR

(see section 2.2.1) could lead to a powerful performing recombinant *A. woodi* strain with the ability to withstand adverse and inhibitory conditions.

Bibliography

[1] M. Adams, L. Mortenson, and J. Chen. Hydrogenase. *Biochim. Biophys. Acta 594 (2-3), 105-176*, 1981.

[2] R. Bache and N. Pfenning. Selective isolation of *Acetobacterium woodii* on methoxylated aromatic acids and determination of growth yields. *Arch. Microbiol. 130 (3):255–261*, 1981.

[3] W. Balch, S. Schoberth, R. Tanner, and R. Wolfe. *Acetobacterium*, a new genus of hydrogen-oxidizing, carbon dioxide-reducing, anaerobic bacteria. *Int. J. Syst. Bacteriol. 27 (4): 355–361*, 1977.

[4] P. Bell and C. Ko. Process for fermentation of syngas- us patent 8592191, 2013.

[5] S. Bernacchi, S. Rittman, A. Seifert, A. Krajete, and C. Herwig. Experimental methods for screening parameters influencing the growth to product yield ($y_{X/CH4}$) of a biological methane production (bmp) process performed with *Methanothermobacter marburgensis*. *AIMS Bioengineering Volume 1, Issue 2, 72-87*, 2014.

[6] J. Bertsch and V. Müller. Bioenergetic constraints for conversion of syngas to biofuels in acetogenic bacteria. *Biotechnol. Biofuels 210 (8)*, 2015.

[7] J. Bertsch and V. Müller. Co metabolism in the acetogen *Acetobacterium woodii*. *Applied and Environmental Microbiology Volume 81: 5949-5956*, 2015.

[8] E. Biegel and V. Müller. Bacterial na$^+$ - translocating ferredoxin:nad$^+$ oxidoreductase. *Proc. Natl. Acad. Sci. USA 107, 18138-18142*, 2010.

[9] Biospectra. *Referenzdokumentation Lucullus PIMS 3.1 Version 3.1.0*, 2009.

[10] R. Boenigk, P. Dürre, and G. Gottschalk. Carrier mediated acetate transport in *Acetobacterium woodii. Arch. Microbiol. 152, 589-593*, 1989.

[11] K. Braun and G. Gottschalk. Effect of molecular hydrogen and carbon dioxide on chemo-organotrophic growth of *Acetobacterium woodii* and *Clostridium aceticum. Arch. Microbiol. 128 (3): 294-298*, 1981.

[12] S. Braus-Strohmeyer, G. Schnappauf, G. Braus, A. Größer, and H. Drake. Carbonic anhydrase in *Acetobacterium woodii* and other acetogenic bacteria. *J. Bacteriol. 179 (22), 7197-7200*, 1997.

[13] H. Chmiel. *Bioprozesstechnik*, volume 3., neu bearbeitete Auflage. Spektrum Akademischer Verlag Heidelberg 2011, 2011.

[14] S. Daniels, T. Hsu, S. Deans, and H. Drake. Characterization of the h2- and co- dependent chemolithotropic potentials of acetogens *Clostridium thermoaceticum* and *Acetogenium kivui. J.Bacteriol. 172 (8), 4464-4471*, 1990.

[15] M. Demler. Reaktionstechnische untersuchungen zur autotrophen herstellung von acetat mit *Acetobacterium woodii*, 2012.

[16] M. Demler and D. Weuster-Botz. Reaction engineering analysis of hydrogenotrophic production of acetic acid by *Acetobacterium woodii. Biotechnology and Bioengineering 108 (2), 470-474*, 2010.

[17] P. Doran. Mass transfer. *Bioprocess Engineering Principles, Elsevier Ltd., Oxford*, 2006.

[18] P. M. Doran. *Bioprocess Engineering Principles*. Elsevier Science & Technology Books, 1995.

[19] H. L. Drake, S. L. Daniel, K. Küsel, C. Matthies, C. Kuhner, and S. Braus-Stromeyer. Acetogenic bacteria: what are the in situ consequences of their diverse metabolic versatilities? *BioFactors 6 (1997) 13–24*, 1997.

[20] P. Dürre and B. J. Eikmanns. C1-carbon sources for chemical and fuel production by microbial gas fermentation. *Biotechnology 2015, 35:63–72*, 2015.

84

[21] EuropeanComission. Magazine setis - strategic energy technologies information system.

[22] J. Fricke. *Optimierung eines Herstellungsprozesses artifizieller Malaria-Vakzine mittels Design of Experiments*, volume Fortschr.-Ber. VDI Reihe 17 Nr. 290. VDI Verlag GmbH, 2015.

[23] M. Fritz and V. Müller. An intermediate step in the evolution of atpases - the f_1f_0- atpase from *Acetobacterium woodii* contains f-type and v-type rotor subunits and is capable of atp synthesis. *FEBS J. 274 (13), 3421-3428*, 2007.

[24] G. Fuchs, E. Thomas, H. Johann, K. Börries, and K. Erika. *Allgemeine Mikrobiologie*, volume 9. Auflage. Georg Thieme Verlag KG, 2014.

[25] B. S. Genthner and M. Bryant. Additional characteristics of one-carbon-compound utilization by eubacterium limosum and acetobacterium woodii. *Appl. and Environ. Microbiol. Vol. 53 (3); p. 471-476*, 1986.

[26] T. E. Gradel and B. R. Allenby. *Industrial Ecology, 2nd Edition*. Prentice Hall, 2003.

[27] R. Heise, V. Müller, and G. Gottschalk. Sodium dependence of acetate formation by the acetogenic bacterium *Acetobacterium woodii*. *J. Bacteriology 171 (10), 5473-5478*, 1989.

[28] R. Heise, J. Reidlinger, V. Müller, and G. Gottschalk. A sodium-stimulated atp synthase in membrane vesicles of the homoacetogenic bacterium *Acetobacterium woodii*. *FEBS Lett. 295:119-122*, 1991.

[29] V. Hess, K. Schuchmann, and V. Müller. The ferredoxin:nad+ oxidoreductase (rnf) from the acetogen *Acetobacterium woodii* requires na$^+$ and is reversibly coupled to the membrane potential. *J. Biol. Chem. 288 (44), 31496-31502*, 2013.

[30] D. H.L., G. A.S., and D. S.L. Old acetogens, new light. *Ann. N.Y. Acad. Sci. 1125: 100-128*, 2008.

[31] M. Holmes and T. Erickson. Ncht tech brief: Hydrogen separation membranes. *www.undeerc.org/ncht (accessed 14.09.2017)*, 2010.

[32] R. Hungate and J. Marcy. The roll-tube method for cultivation of strict anaerobes. *Bull. Ecol. Res. Comm. 17: 123-126*, 1973.

[33] S. Jones, A. Fast, E. Carlson, C. Wiedel, J. Au, M. Antoniewicz, E. Papoutsakis, and B. Tracy. CO_2 fixation by anaerobic non-photosynthetic mixotrophy for improved carbon conversion. *Nature Communications 7, Article number: 12800*, 2016.

[34] C. Kantzow, A. Mayer, and D. Weuster-Botz. Continuous gas fermentation by *Acetobacterium woodii* in a submerged membrane reactor with full cell retention. *Journal of Biotechnology Vol(212): 11 - 18*, 2015.

[35] C. Kantzow and D. Weuster-Botz. Effects of hydrogen partial pressure on autotrophic growth and product formation of *Acetobacterium woodii. Bioprocess Biosyst Eng (2016) 39:1325–1330*, 2016.

[36] C. A. Kantzow. Prozessintensivierung der gasfermentation mit *Acetobacterium woodii* in rührkesselreaktoren, 2015.

[37] A. Karnholz, K. Küsel, A. Gößner, A. Schramm, and H. L. Drake. Tolerance and metabolic response of acetogenic bacteria toward oxygen. *Appl. and Environ. Microbiol., Feb. 2002, p. 1005–1009*, 2002.

[38] leibniz institut DSMZ Deutsche Sammlung für Mikroorganismen und Zellkulturen GmbH. Cultivation of anaerobes, 2017.

[39] L. Ljungdahl. The autotrophic pathway of acetate synthesis in acetogenic bacteria. *Annu. Rev. Microbiol. 40: 415-450*, 1986.

[40] T. L.P. and S. S.D. Fermentation process - us patent 9068202, 2015.

[41] M. Madigan, J. Martinko, D. Stahl, and D. Clark. *Mikrobiologie kompakt*, volume 13., aktualisierte Auflage. Pearson Deutschland GmbH, 2015.

[42] C.-F. Mandenius. *Bioreactors - Design,Operation and Novel Applications.* Wiley-VCH Verlag GmbH & Co KGaA, Germany, 2016.

[43] T. Miller and M. Wolin. A serum bottle modification of the hungate technique for cultivating obligate anaerobes. *Applied Microbiology, May 1974, p. 985-987*, 1974.

[44] T. Miller and M. Wolin. A serum bottle modifictaion of the hungate technique for cultivating obilgate anaerobes. *Appl. Microbiol. Vol. 27, No. 5: 985-987*, 1974.

[45] V. Müller. Energy conservation in acetogenic bacteria. *Appl. Environ. Microbiol. 69 (11), 6345-6353*, 2003.

[46] Y. Nie, H. Liu, G. Du, and J. Chen. Acetate yield increased by gas circulation and fed-batch fermentation in a novel syntrophic acetogenesis and homoacetogenesis coupling system. *Bioresource Technology 99 (2008) 2989–2995*, 2007.

[47] J. Nielsen, J. Villadsen, and G. N. *Bioreaction Engineering Principles.* Kluwer Academic/Plenum Publishers, 2003.

[48] J. Perl. *Sustainability Engineering - A design guide for the Chemical Process Industry.* Springer International Publishing AG Switzerland, 2016.

[49] V. Peters, P. Janssen, and R. Conrad. Efficiency of hydrogen utilization during unitrophic and mixotrophic growth of *Acetobacterium woodii* on hydrogen and lactate in the chemostat. *FEMS Microbiology Ecology (26), 317-324*, 1998.

[50] A. Poehlein, S. Schmidt, A.-K. Kaster, M. Goenrich, J. Vollmers, A. Thürmer, J. Bertsch, K. Schuchmann, B. Voigt, M. Hecker, R. Daniel, R. K. Thauer, G. Gottschalk, and V. Müller. An ancient pathway combining carbon dioxide fixation with the generation and utilization of a sodium ion gradient for atp synthesis. *PLoS ONE 7(3): e33439*, 2012.

[51] S. W. Ragsdale and E. Prize. Acetogenesis and the wood-ljungdahl pathway of co2 fixation. *Biochim Biophys Acta. 1784(12): 1873-1898*, 2008.

[52] S. Rittmann, A. Seifert, and C. Herwig. Essential prerequisites for successful bioprocess development of biological ch_4 production from co_2 and h_2. *Crit. Rev. Biotechnol, Early Online:1-11*, 2013.

[53] H. Sahm, G. Antranikian, K. Stahmann, and R. Takors. *Industrielle Mikrobiologie.* Springer-Verlag Berlin Heidelberg, 2013.

[54] R. Sander. Compilation of henry's law constants for inorganic and organic species of potential importance in environmental chemistry. *Max-Planck Institute of Chemistry*, 1999.

[55] S. Schmidt. Die entschlüsselung des genoms von acetobacterium woodii: neue einblicke in die lebensweise und bioenergetik eines acetogenen bakteriums, 2011.

[56] S. Schmidt, E. Biegel, and V. Müller. The ins and outs of na^+ bioenergetics in *Acetobacterium woodii. Biochimica et Biophysica Acta 1787 (2009) 691–696*, 2009.

[57] K. Schuchmann and V. Müller. Autotrophy at the thermodynamic limit of life: a model for energy conservation in acetogenic bacteria. *Nature Reviews Microbiology: 809–821*, 2014.

[58] A. Seifert, S. Rittmann, and C. Herwig. Analysis of process related factors to increase volumetric productivity and quality of biomethane with *Methanothermobacter marburgensis. Applied Energy 132: 155-162*, 2014.

[59] J. Shin, Y. Song, Y. Jeong, and B.-K. Cho. Analysis of the core genome and pangenome of autotrophic acetogenic bacteria. *Frontiers in Microbiology; September 2016: Vol. 7, Article 1531*, 2016.

[60] M. Straub, M. Demler, D. Weuster-Botz, and P. Dürre. Selective enhancement of autotrophic acetate production withgenetically modified *Acetobacterium woodii. Journal of Biotechnology 178 (2014) 67–72*, 2014.

[61] A. Tschech and N. Pfennig. Growth yield increase linked to caffeate reduction in *Acetobacterium woodii. Arch.Microbiol. 137:163-167*, 1984.

[62] H. Vogel and C. Todaro. *Fermentation and biochemical engineering handbook: Principles, process design and equipment*, volume 2nd Ed Westwood, N.J. Noyes Publications, 1997.

[63] E. Wilhelm, R. Battino, and R. Wilcock. Low-pressure solubility of gases in liquid water. *Chem. Rev. 77 (2): 219-262*, 1977.

[64] H. Wood, S. Ragsdale, and E. Pezacka. The acetyl-coa pathway of autotrophic growth. *FEMS Microbiol, Lett 39 (4): 345-362*, 1986.

[65] B. H. Yan, A. Selvam, S. Y. Xu, and J. W. Wong. A novel way to utilize hydrogen and carbon dioxide in acidogenic reactor through homoacetogenesis. *Bioresource Technology 159 (2014) 249–257*, 2014.

A. Appendix

A.1. Media recipes

Table A.1.: Complex Media DSMZ 135, Copyright 2015 DSMZ GmbH

NH_4Cl	1.00	g
KH_2PO_4	0.33	g
K_2HPO_4	0.45	g
$MgSO_4$ x 7 H_2O	0.10	g
Trace element solution (see medium 141)	20.00	ml
Yeast extract	2.00	g
Na-resazurin solution (0.1% w/v)	0.50	ml
$NaHCO_3$	10.00	g
D-Fructose	10.00	g
Vitamin solution (see medium 141)	10.00	ml
L-Cysteine-HCl x H_2O	0.50	g
Na_2S x 9 H_2O	0.50	g
Distilled water	1000.00	ml

Dissolve ingredients except bicarbonate, fructose, vitamins, cysteine and sulfide, bring to the boil and cool to room temperature under 80% N_2 and 20% CO_2 gas mixture. Add bicarbonate (solid) and equilibrate the medium with the gas until a pH of around 7.4 is reached. Then distribute under the same gas atmosphere in anoxic Hungate-type tubes or serum vials and autoclave. Before use adjust the pH to 8.2 by adding a sterile anoxic stock solution of carbonate (5% w/v) prepared under 80% N_2 and 20% CO_2 gas mixture (c. 0.25 ml per 10 ml medium) and add fructose, vitamins (sterilized by filtration), cysteine and sulfide from anoxic sterile stock solutions prepared under 100% N_2.
Note: For autotrophic growth fructose is omitted and a gas atmosphere of 80% H_2 and 20% CO_2 is used.

Table A.2.: Trace element solution DSMZ 141, Copyright 2015 DSMZ GmbH

Trace element solution:

Nitrilotriacetic acid	1.50	g
$MgSO_4$ x 7 H_2O	3.00	g
$MnSO_4$ x H_2O	0.50	g
NaCl	1.00	g
$FeSO_4$ x 7 H_2O	0.10	g
$CoSO_4$ x 7 H_2O	0.18	g
$CaCl_2$ x 2 H_2O	0.10	g
$ZnSO_4$ x 7 H_2O	0.18	g
$CuSO_4$ x 5 H_2O	0.01	g
$KAl(SO_4)_2$ x 12 H_2O	0.02	g
H_3BO_3	0.01	g
Na_2MoO_4 x 2 H_2O	0.01	g
$NiCl_2$ x 6 H_2O	0.03	g
Na_2SeO_3 x 5 H_2O	0.30	mg
Na_2WO_4 x 2 H_2O	0.40	mg
Distilled water	1000.00	ml

First dissolve nitrilotriacetic acid and adjust pH to 6.5 with KOH, then add minerals.
Adjust final to pH 7.0 with KOH.

Table A.3.: Vitamin solution DSMZ 141, Copyright 2015 DSMZ GmbH

Vitamin solution:

Biotin	2.00	mg
Folic acid	2.00	mg
Pyridoxine-HCl	10.00	mg
Thiamine-HCl x 2 H_2O	5.00	mg
Riboflavin	5.00	mg
Nicotinic acid	5.00	mg
D-Ca-pantothenate	5.00	mg
Vitamin B_{12}	0.10	mg
p-Aminobenzoic acid	5.00	mg
Lipoic acid	5.00	mg
Distilled water	1000.00	ml

Table A.4.: Trace element solution SL9 from [61]

Compound	Concentration	Unit
Nitrilotriacetic acid	12.8	g
$FeCl_2$ x 4 H_2O	2.0	g
$ZnCl_2$	0.07	g
$MnCl_2$ x 4 H_2O	0.1	g
H_3BO_3	0.006	g
$CoCl_2$ x 6 H_2O	0.19	g
$CuCl_2$ x 2 H_2O	0.002	g
$NiCl_2$ x 6 H_2O	0.024	g
Na_2MoO_4 x 2 H_2O	0.036	g
Distilled water	1000	mL

Table A.5.: Selenite-Wolframite solution from [61]

Compound	Concentration	Unit
NaOH	0.50	g/L
Na_2SeO_3	3.0	mg/L
Na_2WO_4	4.0	mg/L

A.2. Standard Operation Procedure- anaerobic chamber

Research Division
Biochemical Engineering

Standard Operating Procedure	Bioprocess Technology
How to use the anaerobic chamber	Page: 1 / 3
SOP Number: XX Status: Effective/Editable	Date: 2017/08/31
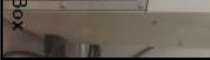
Version	1.0
Replaced version	none
Author	Florian Niederberger, Stefan Pflügl
Date	2017/08/31
Signature	
Authorized by	
Date of authorization	
Signature	

Summary | Description of the anaerobe chamber utilization and how to work inside

Materials
- All materials required for you experiments (Micro-tubes, water, chemicals, vessels, etc...)
- IMPORTANT: do not take inside non-vacuum resistant closed vessels.

Equipment
- Vinyl Anaerobe Chamber/Glove Box (Coy Laboratory Products INC.)
- Gas Bottle (Air Liquide: ARCAL F5 containing 95%N2, 5% H2)
- Vacuum pump

SOP XX – Anaerobic chamber

Research Division
Biochemical Engineering

Standard Operating Procedure	Bioprocess Technology
How to use the anaerobic chamber	Page: 2 / 3
SOP Number: XX Status: Effective/Editable	Date: 2017/08/31

Interruptor   Valve 1   Valve 2   Catalyst Box

Procedure
- Open the gas bottle near the anaerobic chamber.
- Prepare your material you need then put them inside the material sluice.
- Let gas enter the sluice using the small valve (Valve 1) connected on the top of the sluice with the gas tube until the pressure inside reaches ambient pressure (0).
- Open, the door and put inside your materials. Please be sure that every non vacuum resistant bottles are enough opened to allow air to go out.
- Close the door.
- Switch on the vacuum pump (Interrupter) and open the second valve (Valve 2), until vacuum reaches around -25 mmHg.

SOP XX – Anaerobic chamber

Research Division Biochemical Engineering	**Standard Operating Procedure**	**Bioprocess Technology**
	How to use the anaerobic chamber	Page: 3 / 3
	SOP Number XX	Date: 2017/08/31
	Status: Effective/Editable	

- Close the vacuum valve and open the valve for the gas inlet. Be careful to not open on the air entry side.
- Repeat Vacuum/pressurization as least 3 times in total.
- Put your hands inside the gloves and open the sluice from inside the anaerobic chamber.
- Close the door and let ~5 mmHg of vacuum in the sluice to ensure no accidental opening.
- Work inside the chamber.
  - Anaerobize the liquids by stirring them intensive for approximately 20min without a lid.
  - Be aware that the chamber is no sterile environment like the laminar flow.
  - Strictly avoid working with living material (cells, etc.).
  - Research Hungate techniques for proper anaerobic handling and be aware of special needs for your purpose.
- When it's over, open the valve (Valve 2) with the gas pipe until 0 mmHg (Be careful to not open on the air entry side).
- Open the door and put all your stuff inside, close the door.
- Open the door from the outside and get back your stuff.
- Make some Vacuum inside the sluice ~5mmHg.
- Close the gas bottle.
- Use the User Book (blue notebook).

Maintenance:
- Once per month, put the catalyst in the oven at 150°C for regeneration of the catalyst (H_2O evaporation)

Literature:

SOP XX – Anaerobic chamber

V

A.3. Standard Operation Procedure- gas exchange station

Page 1/7

TU VIENNA Technische Universität Wien Vienna University of Technology	Standard Operating Procedure	Change of gas phase in serum bottles with anaerobic gassing station and premixed gases from gas bottles or self-mixed gases	Bioprocess Technology
Research Division Biochemical Engineering		SOP Number: XX Status: Effective/Editable	Date: 2017/08/31 Page: 1 / 7

Version	1.0
Replaced version	none
Author	Florian Niederberger, Stefan Pflügl
Date	2017/08/31
Signature	
Authorized by	
Date of authorization	
Signature	

Summary	Change of gas phase in serum bottles using the gassing manifold and premixed gases from gas bottles or self-mixed gases

Materials
- Sterile filters with luer-lock system
- sterile needles
- EtOH 70 %

Equipment
- Anaerobic gassing station (gassing manifold), including vacuum pump, manometer
- Either connection to premixed gas in bottle (in gas cupboard)
- Or MFCs (amount depending on components in gas mixture) and gas bottles (in gas cupboard)

Procedure

With premixed gas in gas tank
- open valve at gas bottles (#1, figure 1) by turning valve clockwise (gas cupboard next to fermenter lab)

SOP XX - Gas exchange station for anaerobic serum bottles

Page 2/7

TU VIENNA Technische Universität Wien Vienna University of Technology	Standard Operating Procedure	Change of gas phase in serum bottles with anaerobic gassing station and premixed gases from gas bottles or self-mixed gases	Bioprocess Technology
Research Division Biochemical Engineering		SOP Number: XX Status: Effective/Editable	Date: 2017/08/31 Page: 2 / 7

- open connection #2 by turning until red dot turns green
- adjust pressure in line by regulating with #3
- open output of line in the lab (above reactor F6) by turning #4 from 3 o'clock to 12 o'clock (figure 2)
- adjust pressure in line to 1-2 bar by turning #5 (figure 2)

Mix own gas with F7 or F11 (H2, CO2 and air) MFCs gas
- open gas bottles (gas cupboard in fermenter lab) as described before and adjust pressure with (#3, figure 1) to 3bar
- connect the MFCs general output with the gassing manifold station
- set the flow value on the SiemensBoard accordingly to your wanted composition (overall gas flow should be around 1l/min)

- spray EtOH on rubber plug of each bottle
- attach a filter
- use fresh filter every time
- use fresh filter when two or more different cultures will be gassed (risk of contamination!)
- make sure output line is dry and clean (rinse with EtOH and AD and dry when required)
- attach needle to filter attached to the output line of the gassing manifold (#6, figure 3)
- turn on white part of vacuum pump (#7, figure 3)
- put needle in serum bottle, be careful that needle is not in liquid (will be sucked back in line, risk of contamination!)
- adjust line correctly (#8, #9 and #10, figure 3)
- #8 and #10 must always be set to ⊢
- for applying vacuum, #9 must be set to ⊢

SOP XX - Gas exchange station for anaerobic serum bottles

Research Division *Biochemical Engineering*	**Standard Operating Procedure** **Change of gas phase in serum bottles with anaerobic gassing station and premixed gases from gas bottles or self-mixed gases**	*Bioprocess Technology*
SOP Number: XX Status: Effective/Editable		Page: 3 / 7
		Date: 2017/08/31

- turn on vacuum pump (green button) (#11, figure 3)
- turn vacuum pump off when pressure is at ~ -0.5-0.7 bar
- turn #9 to ___
- open valve for gas stream by turning counter-clockwise (# 12, figure 3), be very careful, open valve only by a quarter revolution to avoid too high pressure in line
- turn #9 to ___ to allow flow into bottle when pressure is 0, close valve
- carefully open valve #12 by a quarter revolution, pressurize bottle until 1.5 bar
- open more if necessary to obtain pressure setpoint
- close valve #12
- repeat three times (vacuum-pressurizing)
- apply pressure of 1.5 bar (or required pressure) in the end, close valve
- turn off vacuum pump (#11, figure 3)
- remove needle and filter, discard
- close output of line in the lab (above reactor F6), in reverse direction of opening (#4 and #5, figure 2)
- close gas bottle in the gas cupboard in reverse direction of opening (#1 and #2, figure 1)
- note: closing the gas bottles after use is very important! Bottles will empty with time which is both dangerous and expensive!

Literature
-

Research Division *Biochemical Engineering*	**Standard Operating Procedure** **Change of gas phase in serum bottles with anaerobic gassing station and premixed gases from gas bottles or self-mixed gases**	*Bioprocess Technology*
SOP Number: XX Status: Effective/Editable		Page: 4 / 7
		Date: 2017/08/31

Figure 1: connection of gas bottle in gas cupboard 3. (1) valve at bottle, opens clockwise (2) valve at gas line, open by turning counter-clockwise (dot turns from red to green) (3) adjust pressure in line (increase by turning clockwise, decrease by turning counter-clockwise)

Research Division Biochemical Engineering	Standard Operating Procedure		
TU VIENNA Technische Universität Wien	Change of gas phase in serum bottles with anaerobic gassing station and premixed gases from gas bottles or self-mixed gases	SOP Number: XX Status: Effective/Editable	*Bioprocess Technology*
		Page: 5 / 7	Date: 2017/08/31

Figure 2: (4) turn #4 from „3 o'clock to 12 o'clock". adjust pressure by turning #5 (for increase turn clockwise, for decrease turn counter-clockwise)

SOP XX - Gas exchange station for anaerobic serum bottles

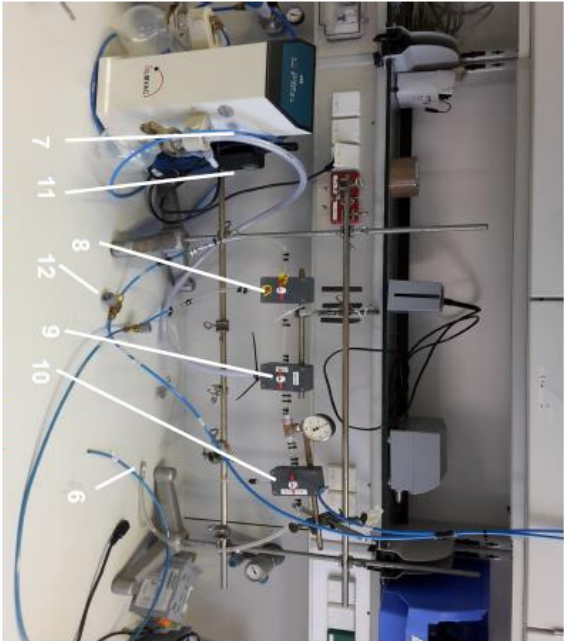| Research Division Biochemical Engineering	Standard Operating Procedure		
TU VIENNA Technische Universität Wien	Change of gas phase in serum bottles with anaerobic gassing station and premixed gases from gas bottles or self-mixed gases	SOP Number: XX Status: Effective/Editable	*Bioprocess Technology*
		Page: 6 / 7	Date: 2017/08/31

Figure 3: anaerobic gassing station (gassing manifold). Use according to description in this SOP. Attention: be careful not to open #12 too much, one quarter revolution in the beginning, adjust when necessary

SOP XX - Gas exchange station for anaerobic serum bottles

Research Division Biochemical Engineering	Standard Operating Procedure	SOP Number: XX	Page:
	Change of gas phase in serum bottles with anaerobic gassing station and premixed gases from gas bottles or self-mixed gases		7 / 7
		Status: Effective/Editable	Date: 2017/08/31

Figure 4: anaerobic gassing station flow scheme (gassing manifold). Use according to description in this SOP.